ESC HEART FAILURE
ESC Heart Failure 2022; **9**: 958–976
Published online 11 February 2022 in Wiley Online Library (wileyonlinelibrary.com) **DOI:** 10.1002/ehf2.13775

REVIEW

Myocardial oedema: pathophysiological basis and implications for the failing heart

Francisco Vasques-Nóvoa[1,2]*, António Angélico-Gonçalves[1,2], José M.G. Alvarenga[1,2], João Nobrega[1,2], Rui J. Cerqueira[1,2], Jennifer Mancio[1,2], Adelino F. Leite-Moreira[1,2] and Roberto Roncon-Albuquerque Jr.[1,2]

[1]*Cardiovascular R&D Center, Faculty of Medicine, University of Porto, Porto, Portugal; and* [2]*Department of Surgery and Physiology, Faculty of Medicine, University of Porto, Al. Prof. Hernâni Monteiro, Porto, 4200-319, Portugal*

Abstract

Myocardial fluid homeostasis relies on a complex interplay between microvascular filtration, interstitial hydration, cardiomyocyte water uptake and lymphatic removal. Dysregulation of one or more of these mechanisms may result in myocardial oedema. Interstitial and intracellular fluid accumulation disrupts myocardial architecture, intercellular communication, and metabolic pathways, decreasing contractility and increasing myocardial stiffness. The widespread use of cardiac magnetic resonance enabled the identification of myocardial oedema as a clinically relevant imaging finding with prognostic implications in several types of heart failure. Furthermore, growing experimental evidence has contributed to a better understanding of the physical and molecular interactions in the microvascular barrier, myocardial interstitium and lymphatics and how they might be disrupted in heart failure. In this review, we summarize current knowledge on the factors controlling myocardial water balance in the healthy and failing heart and pinpoint the new potential therapeutic avenues.

Keywords Heart failure; Myocardial oedema; Cardiac microcirculation; Cardiac pericytes; Cardiac lymphatics; Myocardial interstitium; Extracellular matrix

Received: 12 July 2021; Revised: 27 October 2021; Accepted: 2 December 2021
**Correspondence to: Francisco Vasques-Nóvoa, Department of Surgery and Physiology, University of Porto, Al. Prof. Hernâni Monteiro, 4200-319 Porto, Portugal. Email: fvasquesnovoa@med.up.pt*
Francisco Vasques-Nóvoa and António Angélico-Gonçalves have contributed equally to this work.

Introduction

The adequate compartmentalization of water in the myocardium is essential to maintain normal cardiac function.[1] Despite several mechanisms known to regulate cardiomyocyte and interstitial volume,[2] the myocardium remains particularly susceptible to oedema formation due to its dense microvascular network and high interstitial flow rate.

Myocardial oedema (MO), defined by the accumulation of cardiac water in interstitial and/or intracellular compartments, has been shown to induce cardiomyocyte injury, dysfunction[3–6] and remodelling.[3,4]

The recent introduction of magnetic resonance imaging (MRI) techniques (e.g. myocardial T1 and T2 mapping) has enabled the non-invasive assessment of the extracellular component, namely, the myocardial water content, suggesting that MO negatively affects the prognosis across acute and chronic heart failure (HF).[7–9] Moreover, advances in the understanding of the myocardial microvascular barrier and lymphatics suggest that myocardial fluid balance disturbances are key determinants of the extent and duration of myocardial injury. These aspects may recast MO as a therapeutic target yet to explore in clinical practice.

The present review aims to summarize the current knowledge on the pathophysiological mechanisms of MO formation and their contribution to the disruption of cardiac homeostasis in the failing heart, also discussing future perspectives on therapeutic targeting of MO.

Basic concepts

Myocardial fluid balance and myocardial oedema

To maintain fluid homeostasis, microvascular fluid filtration into the myocardium must be matched by its removal rate via myocardial lymphatic vessels. Microvascular fluid exchange is governed by the Starling principle, expertly reviewed elsewhere,[1,10] summarized by the revised Starling equation:

$$J_V = L_P S\left[(P_C - P_I) - \sigma(\Pi_C - \Pi_G)\right]$$

where L_P is the hydraulic conductivity, S is the filtration surface area, P_C and P_I are the intracapillary (C) and interstitial (I) hydrostatic pressures, σ is the protein reflection coefficient and Π_C and Π_G are the intracapillary and subglycocalyx (G) colloid osmotic pressures, respectively (*Figure 1*). In order to keep a stable interstitial volume (V_I) and defend against oedema formation, several physiological mechanisms counteract primary perturbations in P_C, Π_C and endothelial barrier function—oedema safety factors.[2]

Figure 1 The disruption of myocardial fluid balance in the failing heart. Multiple mechanisms can contribute for oedema formation in the failing heart and are differentially observed in several types of acute and chronic heart failure. Myocardial ischaemia, inflammation and volume overload negatively impact on microvascular barrier function by promoting the glycocalyx degradation and pericyte detachment, resulting in excessive fluid filtration. The resulting increase in interstitial volume and pressure disrupt the extracellular matrix (ECM) architecture, pulling cardiomyocytes away from capillaries and increasing oxygen diffusion distance. Moreover, ECM degradation and high central venous pressure impair lymphatic recruitment and drainage, leading to the accumulation of inflammatory cells, cytokines and metabolic waste products in the myocardial interstitium. Collectively, these mechanisms can impair myocardial contractility and bioenergetics, increase myocardial stiffness and promote cardiomyocyte apoptosis.

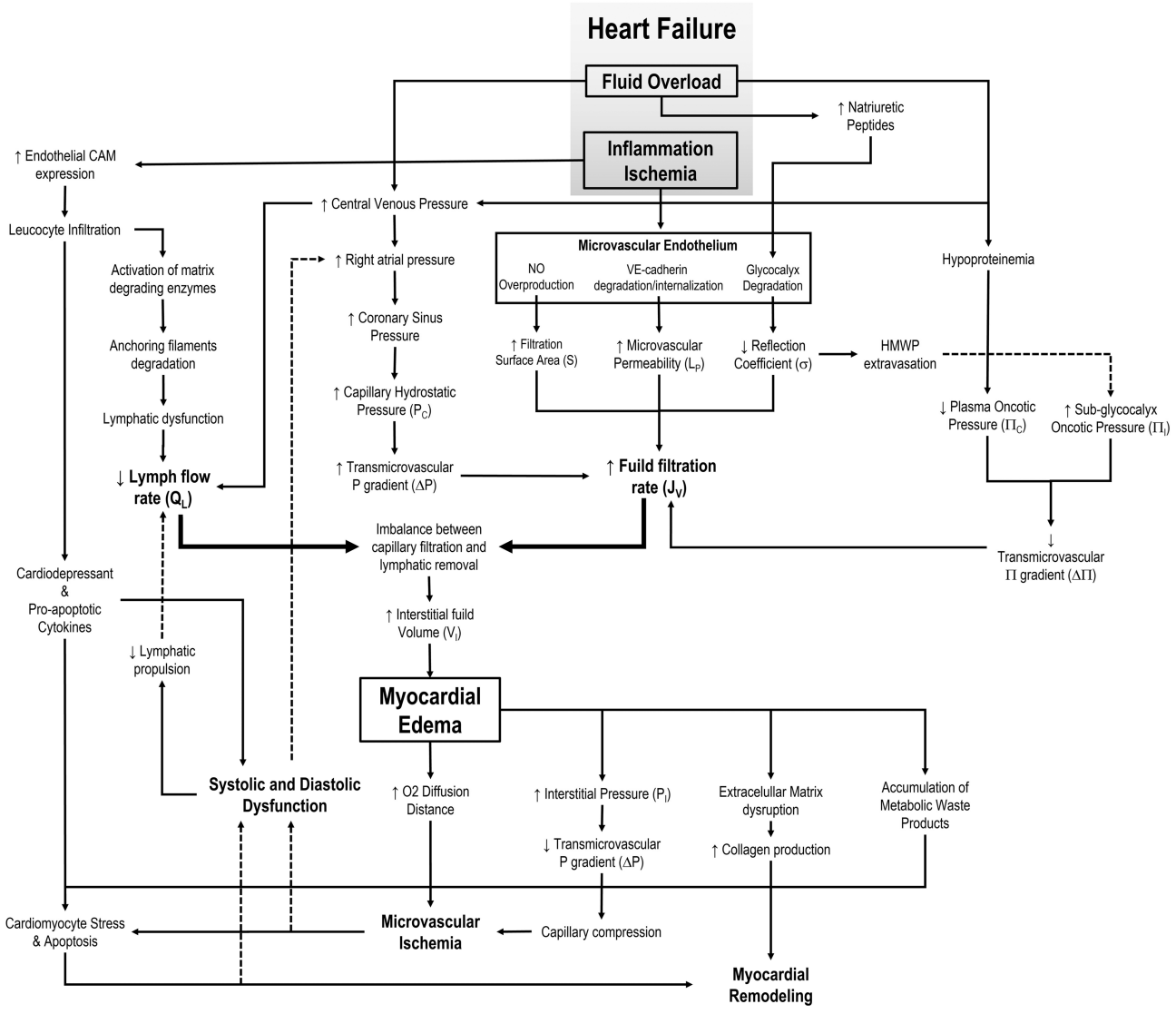

Myocardial oedema develops when fluid filtration rate exceeds lymphatic fluid removal and can be generated by increased ΔP or S, decreased $\Delta\Pi$ or alterations of microvascular membrane properties (increased L_P or decreased σ) (*Figure 1*). Increased P_C can be driven by high pre-capillary pressure in the setting of acute[11] and chronic[12] arterial hypertension, or high post-capillary pressure in coronary sinus occlusion,[4,13,14] pulmonary hypertension[15] or in acute HF with increased central venous pressure.[16] Moreover, increased S, caused by increased capillary recruitment or vasodilation, promotes MO formation and is particularly relevant in inflammatory HF aetiologies (e.g. myocarditis and sepsis). Finally, as albumin is the major determinant of Π_C, states of hypoalbuminemia facilitate fluid filtration and global interstitial oedema.[6] This is particularly relevant in crystalloid coronary perfusion during cardiac surgery[17] and in shock management (e.g. septic and cardiogenic) in which, excessive fluid resuscitation worsens prognosis.[18,19]

Myocardial oedema dramatically reduces energetic efficiency, impairing both contraction and relaxation.[1,20,21] However, increased V_I and P_I have been shown to primarily affect myocardial viscoelastic properties, resulting in higher diastolic stiffness.[6,22] Due to its low interstitial compliance, small interstitial volume expansions create high interstitial pressures, making the myocardium particularly sensitive to oedema formation. The experimental increase in myocardial water content by 3.5% was associated with a 40% drop in cardiac output.[3] In addition, MO directly opposes filtration, by decreasing ΔP and physically compressing the capillaries and disrupting nutrient and oxygen delivery.[23] The disruption of the extracellular matrix structure, increased oxygen diffusion distance and accumulation of metabolic waste products are additional proposed mechanisms of MO-associated functional deterioration (*Figure 2*).[1,24]

In summary, myocardial fluid balance is largely dependent on microcirculation dynamics, microvascular barrier, interstitial architecture and lymphatic drainage. Disruption of any of these components may disturb myocardial fluid homeostasis. In this review, each factor will be addressed in detail regarding its physiological role and how it may be disrupted in the failing heart.

Coronary microcirculation

The healthy myocardium is one of the most densely vascularized tissues in human body, possessing a high density capillary network (3.000–4.000/mm^2) closely disposed around cardiomyocytes[25,26] (*Figure 2*). Such proximity between cardiomyocytes and capillaries is of utmost importance to maintain a short diffusion distance not only for oxygen, but also for potentially toxic byproducts of cellular metabolism.[23] Moreover, the high metabolic rate of the myocardium, which primarily depends on oxidative phosphorylation, translates in an elevated oxygen demand that is matched by a very high oxygen extraction rate (70%–80% in resting conditions).[27–29] Consequently, in stress conditions, additional increments in oxygen demand are predominantly met by parallel increases in myocardial blood flow (MBF).[27] This metabolic contribution to MBF autoregulation is made possible by the close contact

Figure 2 Pathophysiological pathways contributing to myocardial oedema in heart failure.

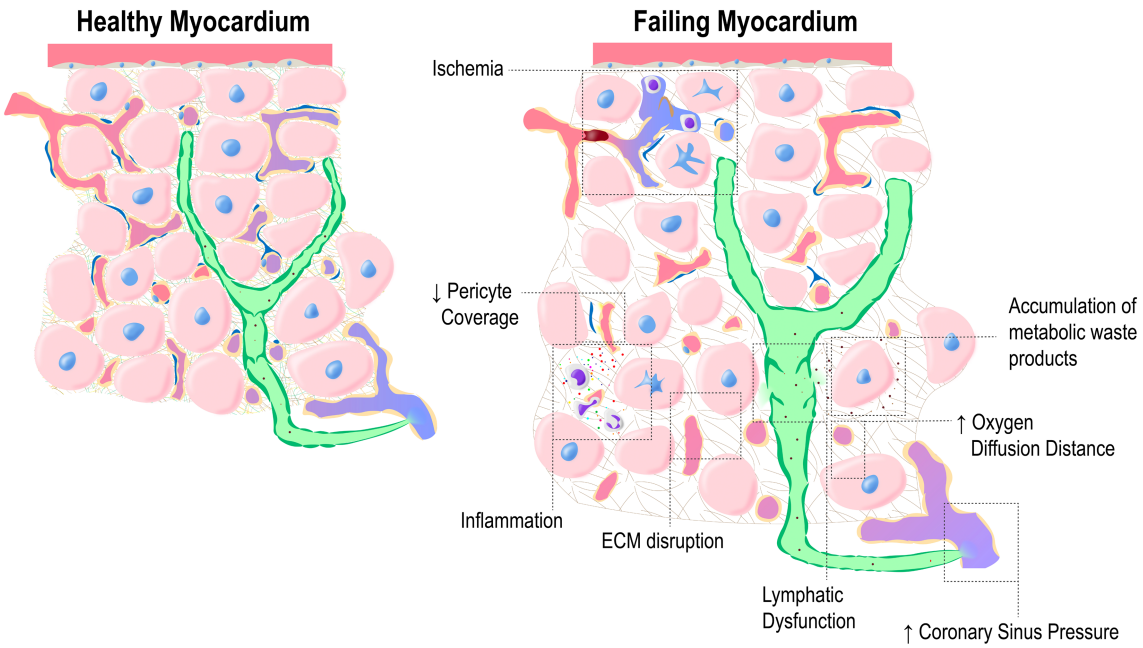

between cardiac muscle and vasculature, enabling cardiomyocyte-derived mediators (CO_2[30] and lactate[31]) and microenvironmental factors (pH[32] and extracellular K^+[33]) to modulate local vasomotor tone and haemoglobin dissociation curve. Therefore, pathological conditions limiting the close communication between cardiomyocytes and vasculature, namely, the expansion of the interstitial space due to oedema or fibrosis, as well as arteriolar and capillary rarefaction, common features in chronic HF,[34] impair diffusional transport and MBF autoregulation, contributing to oxygen supply/demand mismatch (*Figure 2*).

Another consequence of the proximity between coronary microvasculature and cardiomyocytes is their mechanical interaction. Previously considered an important modulator of contractility (i.e. Gregg phenomenon), the effect of coronary perfusion was later shown to be negligible within the autoregulatory pressure-flow range.[35,36] Extravascular forces are not uniform across the ventricular wall and a gradual increase in interstitial pressure and vascular compression is observed from the subepicardium to the subendocardium.[37,38] This is partly compensated by a higher arteriolar density at the subendocardium so that, in physiological conditions, MBF is similar in both myocardial layers.[39,40] Yet, the distinct mechanical cross-talk between different myocardial layers, makes arterio-venous pressure gradient (i.e. perfusion pressure) at the subendocardium about half of that of subepicardium.[41] Consequently, in the setting of decreased coronary pressure (e.g. coronary artery disease), the subendocardial perfusion is predominantly affected.[42–44] This intricate relation between microcirculation and perfusion may underly, at least partially, the existence of clearly distinct patterns of MO distribution associated with different kinds of myocardial injury: in acute inflammatory conditions (e.g. viral myocarditis, sepsis) oedema is generally evident in the subepicardial layers whereas in acute ischaemia, the oedema is transmural or predominantly affects the subendocardium.[7,45–47]

Coronary vasculature also influences myocardial tissue properties. Higher coronary perfusion pressure is associated with increased myocardial stiffness, shifting diastolic pressure-volume relationship left and upwards, even in the absence of oedema formation.[48–50] The underlying mechanism resides in the fact that cardiomyocyte contraction increases the cell diameter, which happens at the expense of coronary vascular diameter, contributing to the abovementioned systolic vascular compression.[36,51] Accordingly, higher intravascular volume and pressure, caused by increased coronary perfusion or venous outflow pressure, oppose intravascular fluid displacement, and therefore impair muscle contraction and relaxation. This has been shown to be especially relevant in the setting of increased coronary sinus pressure, seen in acute and chronic HF, where increased intravascular and interstitial volume act cooperatively to impair systolic function and diastolic compliance.[52–54]

Coronary microvascular barrier

Overlooked in the past, the cardiac microvascular barrier became increasingly recognized as highly active and complex structure, composed of a continuous non-fenestrated endothelial cell monolayer, which is internally coated with a negatively charged gel-like mesh (i.e. glycocalyx) and externally covered by pericytes and basement membrane (*Figure 3*).

Interendothelial junctions

Endothelial cells (EC) are tightly bonded by interendothelial junctions (IEJ), mostly comprised by tight (occludins, claudins and JAMs) and adherens junctions (VE-cadherin), which define endothelial pore size and can be dynamically regulated at the expression level and through internalization, to finely tune endothelial permeability and regulate the passage of macromolecules and cells[55–57] (*Figure 3*). Accumulating evidence suggests IEJ disruption as a potential pathophysiological mechanism in cardiac diseases. Importantly, endothelial expression of claudin-5, a critical player in size-selective barrier function, is reduced in human end-stage HF hearts.[58] This was also shown in experimental diastolic dysfunction induced by western diet, where claudin-5 and occludin down-regulation was associated with increased vascular permeability,[59] an effect attenuated by amiloride, suggesting an important role for endothelial ENaC expression and sodium overload. Regarding adherens junctions, reduced VE-cadherin/β-catenin expression in dilated cardiomyopathy was associated with endothelial cell degeneration,[60] whereas in post-ischaemic MO, Src inhibition prevented VEGF-mediated disruption of Flk/VE-cadherin/β-catenin complex and attenuated post-ischaemic MO, fibrosis and mortality.[61] In addition, key risk factors for HF development and progression have been shown experimentally to promote endothelial hyperpermeability by disrupting EIJ, namely, renin-angiotensin-aldosterone system activation,[62] inflammation,[63,64] hypoxia,[65] cardioplegic arrest,[66] hyperglycaemia,[67] oxidative stress,[68] increased circulating LDL[69,70] and free fatty acid[71] levels.

The endothelial surface layer

The endothelial glycocalyx (eGC) covers the apical side of endothelial cells and consists of a complex meshwork of varied membrane-associated macromolecules[72–74] (*Figure 3*). These include proteoglycans and glycoproteins, forming a backbone in which soluble proteins, plasma- or endothelial-derived, are incorporated. eGC proteoglycans are constituted by linear core proteins, mostly Syndecan-1, to which multiple glycosaminoglycans (GAGs) side chains can be covalently attached.

Figure 3 Molecular interactions in myocardial fluid balance. The myocardium is composed by cardiomyocytes, microvascular capillaries enclosed by pericytes and lymphatic capillaries: fluid is filtrated in microvascular capillaries, through the endothelial surface layer and interendothelial junctions. In the myocardial interstitium, fluid entry is limited by type I and type III collagen fibres and GAGs, extracellular matrix components that act as a buffer for Na^+ and water. Interstitial and intracellular water are in delicate balance, maintained by cardiomyocyte volume regulators. Interstitial fluid (IF) and solutes are collected by initial lymphatic capillaries, enabling a continuous IF renovation, which is returned ultimately to the venous circulation. (A). Cardiomyocyte ionic transporters: cardiomyocytes closely regulate intracellular water entry and extrusion. Water enters through aquaporins or passively diffuses through the cell membrane, according to osmotic gradients established by ionic and solute concentrations. (B). Endothelial cell–pericyte interaction: these cells establish close paracrine and physical (N-cadherin) interactions regulating microvascular stability. Endothelial cells secrete PDGF-BB that binds to PDGFR-β, promoting pericyte recruitment and microvascular integrity, whereas pericytes secrete angiopoietin 1 (Ang-1), which acts on Tie-2 and stabilizes endothelial cells. (C). Endothelial surface layer and interendothelial junction: the endothelial surface layer is composed by endoluminal glycocalyx, which binds plasma proteins and protects endothelial cells. Furthermore, endothelial cells establish varied connections, maintaining cohesiveness and cell survival. (D). Lymph drainage in initial lymphatic capillary: fluid enters the lymphatic vasculature via lymphatic capillaries, which are blunt-ended vessels attached to the extracellular matrix by anchoring filaments. Lymphatic endothelial cells overlap, creating valve-like structures that promote unidirectional lymph flow. These vessels converge progressively from the subendocardium to the subepicardium, forming epicardial lymphatic collectors. ALK-1 and -5, anaplastic lymphoma kinase-1 and 5; Ang-1, angiopoietin-1; AngII, angiotensin II; Aqp, aquaporins; GAG, glycosaminoglycans; HA, hyaluronic acid; JAMs, junctional adhesion molecules; NBS, Na^+/HCO_3^- Symporter; NCX, Na^+/Ca^{2+} exchanger; NHE, Na^+/H^+ exchanger; PDGF-BB, platelet-derived growth factor BB; PDGFR-β, PDGF receptor β; TGF-β, transforming growth factor β; TGFR-β2, TGF receptor β2; Tie-2, angiopoietin-1 receptor.

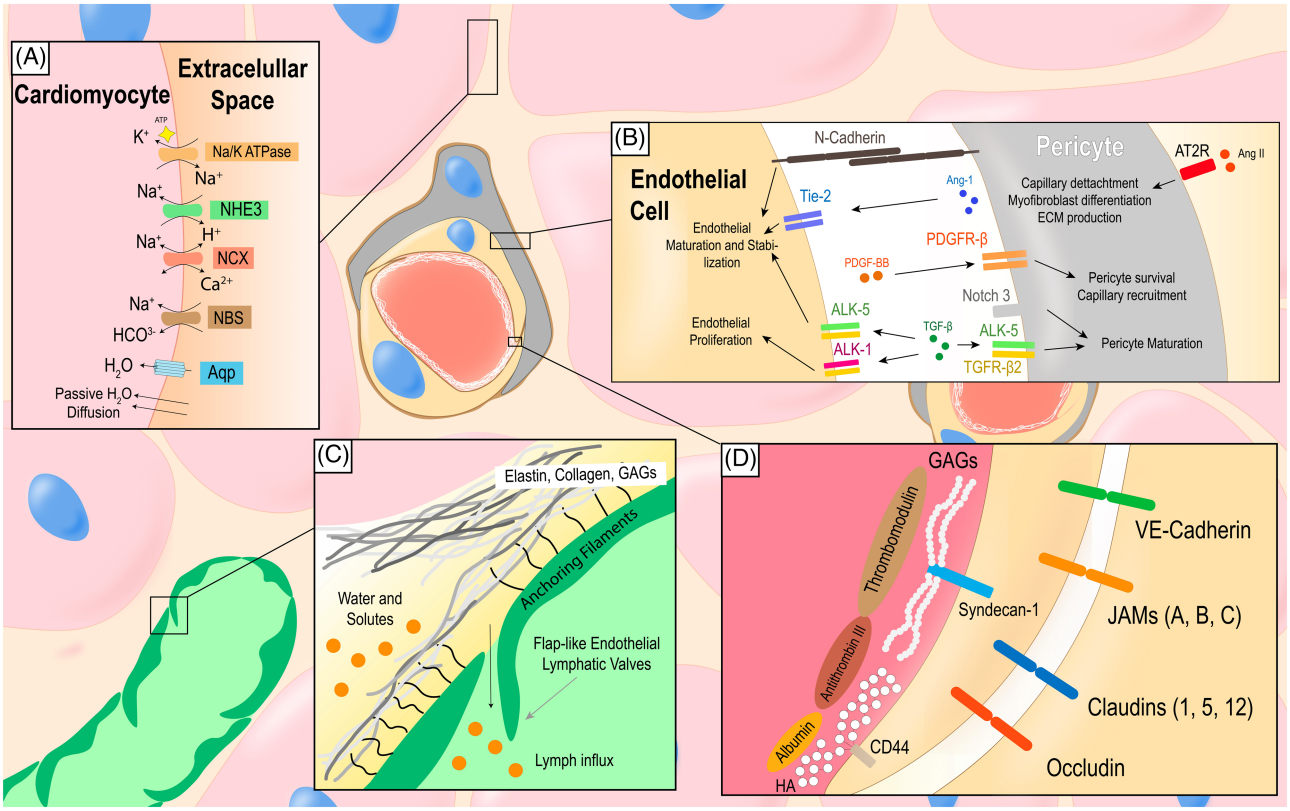

GAGs are highly polyanionic compounds composed of disaccharide repeating units which can be non-sulfated [hyaluronic acid (HA)] or sulfated (chondroitin sulfate, dermatan sulfate, keratan sulfate and heparan sulfate). Together, they form a negatively charged surface that will enable electrostatic interactions with plasma cations, mostly with divalent metal cations (e.g. Ca^{2+}), but also with Na^+ due to its high plasma concentration.[75,76] The resulting high cation concentration at the interface with the plasma enables negatively charged circulating proteins (albumin, antithrombin III and thrombomodulin), that would otherwise not be able to electrically interact with the glycocalyx, to approach and incorporate this layer, forming together the endothelial cell surface layer (ESL).[77,78] The ESL, measuring between 0.2 and 2.0 mm *in vivo*, is therefore a highly complex structure with critical functions in microvascular physiology by (i) physically shielding the underlying endothelium from luminal aggressions; (ii) regulating microvascular flow by transmitting shear-stress forces; (iii) constituting a barrier for plasma proteins and ions, thereby maintaining intravascular oncotic

pressure; (iv) avoiding platelet aggregation by accumulating platelet-inhibitory factors (antithrombin III and thrombomodulin) and physically restricting its interaction with subendothelium at the endothelial gaps; (v) inhibiting endothelial proinflammatory activation (i.e. increased permeability and adhesiveness) by binding circulating cytokines; and (vi) limiting the access and adhesion of circulating immune cells to the EC surface.[79,80,81]

The ESL structure is maintained by a fragile balance between flow and enzymatically mediated shedding, and *de novo* production of its components.[82] Not surprisingly, most pathological mechanisms shown to increase microvascular barrier permeability act concomitantly on IEJ and ESL, namely, in inflammation, ischaemia–reperfusion,[83] hypoxia[84] and hyperglycaemia.[85] Importantly, the activity of glycocalyx-degrading enzymes (i.e. hyaluronidases, heparanase and MMPs) is increased in the setting of inflammation, which, in combination with endothelial CAM overexpression, facilitates leukocyte adhesion and diapedesis.[86] The importance of the permissive effect of ESL degradation on cardiac leukocyte infiltration has been shown in myocardial infarction,[87,88] viral myocarditis[89] and sepsis,[90,91] aggravating the myocardial inflammatory injury. Moreover, degradation of eGC components (hyaluronan[92] and heparan sulfate[93]) has been shown to promote MO by increasing microvascular permeability to water and proteins.

Perhaps, the more striking association between eGC and HF is the fact natriuretic peptides (NP), mostly produced by cardiomyocyte stretching in the setting of hypervolemia and ventricular overload, have been repeatedly shown to promote eGC degradation.[94–98] This effect seems to act concurrently with Na^+ overload, which also leads to the destabilization and collapse of the eGC, mainly through loss of heparan sulfate residues, an effect attenuated by the use of spironolactone.[99] This can be interpreted essentially as a compensatory mechanism, by enabling the escape of excessive intravascular fluid and sodium to the interstitium, which has a high Na^+ buffering capacity due to its GAG content,[100] and acting in conjunction with NP-mediated venodilation to reduce cardiac overload. However, eGC degradation in the setting of myocardial functional impairment might also carry some drawbacks. In addition to eGC degradation being an inherently proinflammatory stimuli for EC,[101,102,103] the impairment of glycocalyx Na^+ buffering capacity may increase the amount of Na^+ presented to the endothelium, promoting intracellular endothelial Na^+ overload and increased transport to the interstitium, resulting in endothelial dysfunction and aggravated interstitial oedema, respectively.[104,105,106] Furthermore, this combined effect of hypervolemia and Na^+ overload also has important implications in the critical care setting (e.g. cardiogenic and septic shock),[107,108] where the frequently excessive crystalloid resuscitation might disrupt microvascular barrier function and complicate haemodynamic management and prognosis. Despite its proposed pathophysiological importance, a direct observation of ESL disruption in HF is still lacking.

Cardiac pericytes

Cardiac pericytes (CPc) are a highly heterogeneous population of perivascular contractile cells that ensheath and intimately interact with underlying endothelial cells, forming a microvascular syncytium.[109,110] Despite conflicting reports, recent data suggest that CPc cover up to 99% of the length of the myocardial microvasculature.[111] CPc share the basement membrane with EC and establish numerous physical interactions, ensuring an adequate control of microvascular permeability. Moreover, an intense reciprocal communication between CPc and EC takes place through gap junctions and paracrine factors, which has been shown to be especially relevant for angiogenesis and stabilization of newly formed vessels[101] (*Figure 3*). Importantly, multiple pericyte phenotypes with distinct cell-surface marker signatures and variable expression of contractile proteins have been shown to be differentially distributed across the arteriolar, microvascular and venular sections of coronary vasculature.[99,112] Such diversity probably underlies distinct pathological roles attributed to pericytes in the context of myocardial injury and remodeling.

Extensive evidence supports a key role for CPc in the regulation of myocardial microvascular flow and permeability. Indeed, the disruption of key trophic and homeostatic pathways for CPc, namely, PDGF-BB/PDGFR-β,[113,114] Ang-1/Tie2,[115,116] Sirtuin-3[117,118] and Notch3,[119,120] has been shown to decrease CPc density and EC coverage, resulting in increased microvascular permeability in response to injury, MO and functional impairment. Importantly, common observations in genetic and drug-induced CPc dysfunction are increased microvascular tortuosity and decreased coronary reserve in response to vasodilator challenge, with cardiac up-regulation of hypoxia-related genes.[121] In knockout mouse models, the genetic ablation of Notch3[122] and Sirtuin-3[123] impairs microvascular maturation and pericyte/EC interaction, exacerbating ischaemic injury and hindering post-ischaemic functional recovery. Similar observations were made in experimental models of endotoxemia and diet-induced obesity, in which Sirtuin-3 has been shown to be down-regulated.[124,125] Accordingly, in the setting of ischaemic injury, cardiomyocyte-derived proNGF activates p75 neurotrophin receptor, causing pericyte process retraction, resulting in a lack of support of the microvascular endothelium and perivascular oedema.[126] Moreover, Hypoxia-Induced Endoplasmic Reticulum Stress Regulating (HypER) lncRNA, which promotes pericyte proliferation, viability and interactions with EC, is down-regulated in human HF,[127] supporting pericyte degeneration as a potentially important pathophysiological mechanism.

In line with the diversity of CPc phenotypes and functional roles in the setting of myocardial ischemia, CPc have also been implicated in the no-reflow phenomenon.[128] Importantly, some pericyte subpopulations express variable amounts of myosin and actin isoforms (α-SMA and γ-actin), having the ability to contract and relax in response to multiple paracrine factors (catecholamines and adenosine).[129,130] Being circumferentially disposed around capillaries, CPc contraction can decrease microvascular flow and theoretically reduce capillary luminal diameter enough to impede the passage of leukocytes. Indeed, in an ischaemia/reperfusion injury model, post-ischaemic capillary blockage sites have been shown to be disproportionally close to pericytes, suggesting ischemic CPc contraction, probably mediated by an increase in intracellular Ca^{2+},[131] as an important mediator of impaired reoxygenation of ischemic tissue following myocardial revascularization.[132]

In inflammatory conditions, CPc detachment from EC surface was associated with differentiation into myofibroblasts and increased production of ECM, potentially contributing to pathological myocardial remodelling.[134,135] In fact, galectin-3, a well-validated biomarker and mediator of cardiac fibrosis in HF patients,[136] has been shown to stimulate pericyte proliferation and procollagen I secretion.[137] This is in accordance with observations in angiotensin II-induced myocardial hypertrophy model, in which $Gli1^+$ cells were shown to consist in a subpopulation of pericytes that, in the setting of injury, differentiate into myofibroblasts and produce ECM in perivascular and interstitial spaces.[138] Further supporting this role of CPc, in a clinically relevant rat model of HF with preserved ejection fraction (ZSF1 obese rats), decreased EC coverage was associated with subendocardial foci of CPc proliferation, which colocalized with ECM deposition and inflammatory cell infiltration.[139] Consistently with this finding, pericytes have been shown to respond to proinflammatory stimuli with overexpression of cytokines, chemokines and CAMs,[140] regulating immune cell diapedesis.[141] In the setting of experimental sepsis, inflammatory-mediated CPc loss facilitates the infiltration of immune cells in cardiac interstitium.[142] These findings highlight the fact that, beyond being key determinants in the microvascular barrier, pericytes may detach from endothelial cells and promote interstitial remodelling in inflammatory injury.

Myocardial interstitium

The myocardial interstitium is a highly organized and compact structure, comprised by fibrillar collagen, non-collagen matrix proteins, proteoglycans, GAGs and a wide array of bioactive signalling molecules[143] (*Figure 3*). Cardiomyocytes are enclosed in a basement membrane, mostly constituted by integrins, laminin and fibronectin, behaving as anchoring points for fibrillar collagen and other matrix components (proteoglycans and GAG) attachment. Collagens (type I and III) are the predominant components of cardiac ECM, and their high tensile strength is assumed to be the main contributor for ECM structural integrity.[144] Cardiac ECM architecture enables an effective force summation of individually contracting cardiomyocytes, allowing a coordinated myocardial tissue contraction, while at the same time maintaining adequate spatial relationships between cells, which prevents cardiomyocyte overstretching, preserves intercellular connections and opposes microcirculatory collapse.

Cardiac ECM composition is an important determinant of interstitial space volume and pressure. The interstitial space is densely crowded with intertwined components, which occupy the available physical space and limit the entrance of plasma proteins or cells, a phenomenon called steric interstitial exclusion.[2] Given their polyanionic nature, interstitial GAGs futher contribute to limit the entrance of plasma proteins, while also binding free ions (mostly Na^+) and annulling their osmotic force.[93] Interestingly, changes in sulfated GAG conformation are associated with decreased Na^+ buffering capacity and interstitial oedema.[93] Moreover, the high stiffness of cardiac ECM not only preserves cardiomyocyte function by generating passive tension and avoiding tissue overstretching but also confers a low interstitial compliance to the myocardium and opposes interstitial space expansion.[145] Consequently, in the setting of increased transcapillary filtration, interstitial fluid (IF) buildup stretches the ECM, causing a steep increase in interstitial pressure, which, in turn, forces IF into the lymphatic system.[22]

Alterations in ECM architecture or composition critically influence myocardial function. Increased ECM deposition, mainly in the form of collagen, has been recognized as an important mechanism of increased stiffness and diastolic dysfunction in most forms of chronic HF.[16] However, mechanical and enzymatic disruption of the ECM also significantly impairs myocardial systolic and diastolic function by compromising force transmission by displacing collagen struts from their anchoring points and breaking intercellular connections.[146,147] Moreover, inflammation-driven up-regulation of ECM-degrading enzymes promotes both ECM and basement membrane degradation, decreasing interstitial exclusion effect and facilitating the interstitial passage of fluid, proteins and immune cells.[148] ECM degradation has been shown in acute high-grade myocardial inflammation, especially in experimental myocarditis[149] and sepsis,[150] where a significant acute decrease in total myocardial collagen content and collagen degradation were observed and associated with MO, systolic and diastolic dysfunction. Further supporting this experimental observation, post-mortem evaluation of human septic myocardium found significant ECM disruption and interstitial oedema at the subepicardium, which colocalized with macrophage infiltration and cardiomyocyte apoptosis.[45] Importantly, disruption of collagen struts may also increase coronary microvasculature suscepti-

bility to external compression, which might compromise MBF in the setting of oedema-associated increased interstitial pressure.[36,123]

Interestingly, chronic oedematous states produced by increased microvascular filtration or decreased lymphatic drainage are associated with increased myocardial collagen deposition.[3,4] The interstitial remodelling may be interpreted as a compensatory mechanism, by decreasing interstitial compliance and preventing interstitial expansion, therefore minimizing the disruption of cardiac architecture. However, increased collagen deposition also causes long-term detrimental effects on overall myocardial compliance and function.[151]

Impaired turnover of non-collagen ECM elements can also promote fibrosis and have detrimental effects on myocardial function. HA is observed in healthy cardiac ECM in its high-molecular-weight HA form and has a unique capacity to bind and retain water molecules.[152] Interestingly, while eGC HA degradation has been consistently associated with endothelial dysfunction, increased microvascular permeability and MO,[85,153] cardiac interstitial accumulation of HA, has similarly been shown to promote MO and structural remodelling.[154] Cardiac interstitial accumulation of HA is normally associated with increased interstitial water content and MO, and is observed in myocardial infarction,[155] hypertrophic cardiomyopathy,[156] myocarditis[157] and experimental cardiac transplant rejection.[158,159] Curiously, hyaluronidase treatment was able to decrease MO in rejected heterotopic transplants,[160] whereas accumulation of low-molecular-weight HA (LMWHA) in hypertrophic cardiomyopathy is not associated with increased water content,[161] raising the possibility of distinct contributions of high-molecular-weight HA and LMWHA for oedema generation. Indeed, in the setting of inflammation and myocardial injury, production of LMWHA is preponderant and has been shown to stimulate TLR inflammatory signalling pathways.[127] Collectively, these results underscore the importance of GAG structure, composition and regional distribution for IF balance.

Cardiac lymphatic system

The cardiac lymphatic system is essential in maintaining myocardial fluid balance and immunological homeostasis.[139] It represents the main route for the removal of cellular metabolites, allowing the continuous IF renewal while avoiding the buildup of interstitial volume and pressure.[2] Additionally, an immunomodulatory role has also been attributed to cardiac lymphatics due to the washout of proinflammatory mediators and immune cells from the myocardial interstitium in the setting of myocardial injury.[162,163]

Lymphatic capillaries are highly specialized blind-ended structures, composed by oak-leaf shaped lymphatic endothelial cells (LEC), which mostly lack basement membrane and are connected by permeable flap-like intercellular junctions that favour unidirectional passage of IF, solutes and immune cells[164,165] (*Figure 3*). Moreover, cardiac LEC are connected to the surrounding ECM and cardiomyocytes by structures designated as anchoring filaments, constituted by type VII collagen projections, integrins and focal adhesion kinases. Anchoring filaments maintain lymphatic patency by exerting tensile forces and opening the lumen of lymphatic capillaries, facilitating lymphatic flow.[166,167] Anatomically, the lymphatic capillary plexus progressively converges from the subendocardium to the subepicardium, suffering structural alterations along the way, namely, the appearance of a continuous basement membrane, intraluminal valves to promote unidirectional flow, tight junctions, and, in larger trunks outside the myocardium, an adventitial layer and surrounding smooth muscle cells to help pump lymph.[168,169] Subepicardial lymphatic pre-collectors converge to form epicardial lymphatic collectors that transport cardiac lymph via lymph nodes towards thoracic ducts, ultimately draining into the superior vena cava.[170]

Several factors influence cardiac lymph flow, most of which known to be unique to the heart. A distinctive feature of the intramyocardial lymphatic system is the absence of smooth muscle in intramyocardial vessels. Therefore, lymph flow is highly dependent on external forces, namely, muscle contraction and deformation along the cardiac cycle, heart rate and contractility.[1] However, factors not intrinsic the heart function also impact lymph drainage. By concentrating interstitial metabolic products and proteins, lymph oncotic pressure exceeds interstitial oncotic pressure, promoting water osmotic dragging and fluid drainage.[1] Coronary venous pressure is also an important regulator of lymph flow. Experimental coronary sinus blockade increases capillary hydrostatic pressure and promotes fluid filtration upstream, which requires compensatory lymphatic dilation and increased lymph flow to maintain fluid homeostasis.[13,14,147] On the other hand, downstream, because lymph is ultimately drained into the venous circulation, increased central venous pressure acts synergically with decreased contractility to impair lymph flow in acute HF, promoting MO.[16,93]

The frequent observation of MO in several aetiologies of HF suggests that cardiac lymphatic inability to respond to increased filtration is a rather common finding. Despite the recognized ability of the healthy heart to respond to an increased capillary filtration by increasing lymph drainage severalfold,[1] multiple disease mechanisms may render the cardiac lymphatic system incapable to cope. In this setting, lymphatic dysfunction will not only promote accumulation of a protein-rich IF, which contributes to microvascular and cardiomyocyte stress, but will also have a proinflammatory effect by decreasing the clearance of proinflammatory cytokines and immune cells.[171] Prolonged residence of cellular debris, inflammatory mediators and cells in myocardial interstitium will aggravate and prolong myocardial

inflammation, especially in the setting of myocardial infarction and myocarditis.[172] Furthermore, the distortion of interstitial architecture mediated by oedema and the activation of collagen and GAG-degrading enzymes may have a negative impact on anchoring filaments and initial lymphatics, further compromising lymphatic patency and function. Whereas acute lymphatic obstruction leads to oedema, chronic obstruction is associated with interstitial fibrosis and ECM remodelling.[125] Moreover, given the close proximity of the lymphatic and electrical conduction system, lymphatic dysfunction has also been shown to be associated with electrical disturbances.[173]

Lymphangiogenesis, the process of producing new lymphatic vessels is known to be a dynamic process mainly regulated by VEGF-C and VEGF-D binding to lymphatic-specific receptor VEGFR3, and to be affected by inflammation and other cardiovascular factors (diabetes and obesity).[146] In acute inflammation[174] and in myocardial infarction,[175] higher fluid filtration increases the need for lymph drainage, with resulting up-regulation of lymphangiogenic factors. However, this endogenous response appears to be insufficient and to result in deficient lymphangiogenesis, with a predominance of lymphatic capillaries and lack of pre-collectors. In fact, in post-infarct mouse models, stimulating lymphangiogenesis with exogenous VEGF-C or adrenomedullin increases lymph flow, decreases MO, attenuates myocardial inflammation and fibrosis and improves cardiac function.[176–180] Still, this promising therapeutic avenue has been recently questioned by the absent impact of genetic blockade of lymphangiogenesis on cardiac function after experimental myocardial infarction.[181]

Cardiomyocyte volume regulation

The cardiomyocyte membrane is highly permeable to water, which moves passively according to osmotic gradients and directly sets cell volume.[182] Normal cell function requires a stable volume and excessive water entry may disrupt membrane and cytoskeleton integrity. To prevent abrupt cell volume alterations, intracellular osmolarity is highly controlled, either with active ionic fluxes or the synthesis/degradation of osmotically active solutes[39,183] (*Figure 3*).

In the isotonic steady-state, intracellular osmotic pressure exceeds extracellular osmotic pressure due to celullar concentration of organic phosphates and proteins, thus favouring passive water entry. To maintain the volume constant, the membrane Na^+/K^+ ATPase promotes the exit of 3 Na^+ and entry of 2 K^+ ions, a phenomenon known as the 'Pump and Leak' concept. Together with low Na^+ membrane permeability, both mechanisms contribute to maintain a low intracellular [Na^+] and a constant transmembrane gradient, on which many ionic transporters that regulate cell volume are highly dependent. In myocardial ischaemia, Na^+/K^+ ATPase dysfunction results in extracellular accumulation of K^+, intracellular accumulation of lactate, Na^+ and Cl^- and consequent cell swelling and membrane depolarization.[159,160] Furthermore, anaerobic metabolites accumulate in extracellular and intracellular spaces. Following reperfusion of the coronary vessels will re-establish water delivery and wash out extracellular, but not intracellular, metabolic products, creating an osmotic gradient that promotes cell swelling. Highlighting the pathophysiological importance of cardiomyocyte oedema in ischaemia/reperfusion injury, reperfusion with a hypertonic solution limited MO and infarct size, when compared with isotonic solution.[184,185]

Cell swelling depolymerizes actin filaments and disrupts cytoskeleton interactions with membrane proteins.[159] Of note, cardiomyocyte swelling induced by ischaemia–reperfusion injury was associated with variable degrees of mitochondrial damage, cytoskeleton abnormalities and significant increases in sarcomere length, radial distance between myofibrils and distance between mitochondria and myofibrils, repercussing on maximal tension and calcium sensitivity.[186] Accordingly, swelling of isolated cardiomyocytes induced by hypotonic medium was associated with lower contractility and activated NO/cGMP/PKG pathway.[158]

Despite most of myocardial water being confined to the intracellular compartment, few studies have addressed the pathophysiological role of cardiomyocyte swelling in HF.

Clinical perspective

In clinical research and practice, MRI stands out as the gold-standard method for non-invasive MO evaluation, based on its ability to identify the tissue 'free' water pool. 'Free' water molecules rotate very rapidly when subjected to a magnetic field and produce long T1 and T2 relaxation times, whereas 'bound' water molecules have their motion restricted due to hydrogen bonding with macromolecules, producing short T2 relaxation time values. The recent introduction of parametric mapping techniques—T1, T2 and extracellular volume, has enabled the detection of subtle changes in myocardial free water content and precise estimation of the interstitial fraction volume and composition.[187]

Making use of aforementioned MRI capabilities, evidence supporting the disruption of myocardial water balance has been shown in a broad range of cardiac and systemic diseases (*Table 1*). Overall, the increase in myocardial free water content is generally associated with depressed left ventricular function, increased NP plasma levels, disease progression and severity, and poor prognosis (*Table 1*). Nevertheless, due to the observational nature of these studies, a causal association between the presence of MO, LV dysfunction and cardiac prognosis could not yet be drawn.

Table 1 Magnetic resonance imaging evidence of myocardial oedema in cardiac and systemic diseases

Disease	Myocardial oedema	CMR imaging	Analytical associations[a]	Clinical associations[a]	References
Acute heart failure	Global	T2 mapping	—	(+) PAWP (−) Decongestion	16,188
Myocardial infarction/ Ischaemia–reperfusion	Focal	T2-weighted imaging, T1, T2 and ECV mapping	(+) Troponin	(+) Infarct extension (+) MACE (+) LV dilatation (−) LV function	189,190
Aortic stenosis	Global	T1 and T2 mapping	—	—	191
Cardiomyopathies					
Non-ischaemic dilated cardiomyopathy	Global	T2-weighted imaging, T2 mapping	—	(−) LVEF (+) Disease progression	192,193
Hypertrophic cardiomyopathy	Focal	T2-weighted imaging, T2 mapping	(+) Troponin (+) BNP	(+) Risk of Syncope	194,195
Takotsubo cardiomyopathy	Focal	T1 and T2 mapping (USPIO enhancement)	(+) Myocardial macrophages	—	196,197
Peripartum cardiomyopathy	Global	T1 and T2 mapping	—	(−) LVEF	198
Infiltrative diseases					
Cardiac amyloidosis	Global	T2 and ECV mapping	(+) NT-proBNP	(+) Mortality (AL)	199
Cardiac sarcoidosis	Focal	T1 and T2 mapping	—	—	200,201
Fabry disease	Focal	T1 and T2 mapping	(+) Troponin	(+) ECG Changes (+) Clinical worsening	202
Infectious diseases					
Viral myocarditis	Focal, subepicardial	T2-weighted and LGE imaging, T2 mapping	(+) Troponin	(+) Arrhythmia (+) MACE (+) Death	9,203–205
COVID-19	Focal	T2-weighted and LGE imaging, T2 mapping	(+) Troponin (+) EMB macrophages	—	206–209
Sepsis	Focal	T2-weighted imaging	—	—	45,210
HIV	Global	T2-weighted and LGE imaging, T1 mapping	—	(+) Adverse cardiovascular events	211
Chagas disease	Focal	T2-weighted and LGE imaging	—	(+) Disease severity	212
Inflammatory diseases					
Rheumatoid arthritis	Focal	T1 and ECV mapping	—	(+) Disease activity (−) Circumferential Strain	213
ANCA-associated vasculitides	Diffuse	T1 and T2 mapping	—	—	214,215
Systemic sclerosis	Focal	T1 and T2 mapping	—	(+) Cold pressor test (+) Disease activity (−) Circumferential Strain	216,217
Systemic lupus erythematosus	Focal	T1 and T2 mapping	—	(+) Disease activity	218,219
Endocrine diseases					
Acromegaly	Global	T2 mapping	—	(+) Reversal of acromegalic cardiomyopathy	220
Hypothyroidism	Global	T2-weighted and LGE imaging, T1 mapping	(−) FT3	(−) Stroke volume (−) Cardiac index	221
Cardiac surgery					
Cardiac transplant	Global	T1 and T2 mapping	—	(+) Transplant rejection	222,223
Systemic diseases and others					
Pulmonary arterial hypertension	Focal	T1 and ECV mapping	—	(−) RV function (+) RV dilatation	224
Chronic kidney disease	Global	T1 and T2 mapping	(+) Troponin T	(+) Uremic Cardiomyopathy	225–228

(*Continues*)

Table 1 (continued)

Disease	Myocardial oedema	CMR imaging	Analytical associations[a]	Clinical associations[a]	References
Breast cancer chemotherapy (Anthracyclines/Trastuzumab)	Focal	T2 mapping	(+) NT-proBNP —	(+) Predictor of cardiotoxicity	229

[a]Positive (+) and negative (—) associations with myocardial oedema.
AL, amyloid light-chain; ECV, extracellular volume; EMB, endomyocardial biopsy; FT3, free triiodothyroinine (T3); LV, left ventricule; LVEF, left ventricular ejection fraction; MACE, composite of total death, myocardial infarction, coronary revascularization, stroke and hospitalization; PAWP, pulmonary arterial wedge pressure; RV, right ventricule; USPIO, ultra-small particles of iron oxide

Myocardial oedema has been particularly well-studied in the acute setting of ischemic heart disease, in which it may have a role on early injury during reperfusion and also late tissue healing.[165–171] During the initial phase of reperfusion, MO may contribute to the pathophysiological process of microcirculation compression and perfusion defects underlying the 'no-reflow' phenomenon.[171,172] MO is also detectable later, at the time of tissue healing and collagen deposition,[166] which discloses the complex interplay between myocardial fluid balance and inflammation and underscores the need for a cautious interpretation of MRI assessment of infarcted and at-risk myocardium.[171,173] Interestingly, patient comorbidities might impact on the development of MO in a disease-specific and somewhat unpredicted way, underscoring the lack of clinical knowledge on this topic. As an illustration, diabetes was shown to aggravate post-ischaemic MO,[174,175] whereas the opposite effect may be present in Takotsubo cardiomyopathy.[176]

Myocardial oedema has not been evaluated as an endpoint in HF randomized clinical trials, and the effect of most drugs on myocardial fluid balance is currently unknown. However, pre-clinical evidence supports the beneficial effect of spironolactone[92] and SGLT2 inhibitors[177] by protecting endothelial glycocalyx. Interestingly, these two drug classes were shown to provide clinical benefit across a wide ejection fraction range in HF,[178–181] supporting a possible role for myocardial fluid balance among their mechanisms of action. Other drugs have proved useful to protect microvascular barrier in distinct clinical scenarios and may oppose MO formation. Of note, aprotinin, a fibrinolysis inhibitor, preserves adherens junctions and reduces MO in experimental cardioplegic arrest,[65] whereas in sepsis, hydrocortisone[182] and sulodexide, a mixture of GAGs (heparan and dermatan sulfates),[183] may protect the glycocalyx and diminish oedema formation.

In contrast, some drugs may facilitate the development of MO by impacting on microvascular filtration and ESL preservation. NP are known disruptors of the ESL[89,91] and BNP levels correlate with myocardial water content across several clinical scenarios (*Table 1*), an association not yet known to be causal. However, it is tempting to speculate that this effect might have contributed to the somewhat disappointing results of BNP analogue nesiritide in the setting of acute HF treatment.[184] In line with this, neprilysin is a known regulator of microvascular permeability by increasing the half-life of NP and bradykinin,[185] suggesting that sacubitril may also perturb microvascular barrier function.[230] Preclinical evidence suggests that beta-blockers[186] and calcium channel blockers[187] may increase microvascular permeability, an effect not yet observed in the myocardium.

Finally, experimental data suggest that stimulators of lymphangiogenesis (e.g. VEGF-C and adrenomedullin) may accelerate oedema resolution after myocardial

infarction,[152,231] but clinical studies are needed before considering this therapeutic pathway in HF.

Conclusion

In the failing heart, myocardial fluid balance is disrupted due to alterations in microcirculation dynamics, microvascular barrier, extracellular matrix composition and lymphatic function. Experimental data suggest that MO significantly impairs cardiac performance, affecting systolic and diastolic properties and promoting long-term adverse remodelling. In the last decade, CMR has been increasingly used for HF phenotyping and data suggest the increase in myocardial free water content as relevant pathophysiological mechanism of cardiac injury and dysfunction, also representing an important prognosticator across multiple cardiac and systemic diseases. The recent advances in the knowledge of microvascular barrier and lymphatic function open the prospect for novel therapeutics targeting myocardial fluid disturbances in HF.

Funding

This study was funded by national funds through FCT - Portuguese Foundation for Science and Technology, under the scope of the Cardiovascular R&D Center – UnIC (UIDB/00051/2020 and UIDP/00051/2020).

References

1. Dongaonkar RM, Stewart RH, Geissler HJ, Laine GA. Myocardial microvascular permeability, interstitial oedema, and compromised cardiac function. *Cardiovasc Res* 2010; **87**: 331–339.
2. Wiig H, Swartz MA. Interstitial fluid and lymph formation and transport: physiological regulation and roles in inflammation and cancer. *Physiol Rev* 2012; **92**: 1005–1060.
3. Laine GA, Allen SJ. Left ventricular myocardial edema. Lymph flow, interstitial fibrosis, and cardiac function. *Circ Res* 1991; **68**: 1713–1721.
4. Desai KV, Laine GA, Stewart RH, Cox CS, Quick CM, Allen SJ, Fischer UM. Mechanics of the left ventricular myocardial interstitium: effects of acute and chronic myocardial edema. *Am J Physiol Heart Circ Physiol* 2008; **294**: H2428–H2434.
5. Rubboli A, Sobotka PA, Euler DE. Effect of acute edema on left ventricular function and coronary vascular resistance in the isolated rat heart. *Am J Physiol* 1994; **267**: H1054–H1061.
6. Miyamoto M, McClure DE, Schertel ER, Andrews PJ, Jones GA, Pratt JW, Ross P, Myerowitz PD. Effects of hypoproteinemia-induced myocardial edema on left ventricular function. *Am J Physiol* 1998; **274**: H937–H944.
7. Friedrich MG. Myocardial edema—a new clinical entity? *Nat Rev Cardiol* 2010; **7**: 292–296.
8. Raman SV, Simonetti OP, Winner MW, Dickerson JA, He X, Mazzaferri EL, Ambrosio G. Cardiac magnetic resonance with edema imaging identifies myocardium at risk and predicts worse outcome in patients with non-ST-segment elevation acute coronary syndrome. *J Am Coll Cardiol* 2010; **55**: 2480–2488.
9. Aquaro GD, Ghebru Habtemicael Y, Camastra G, Monti L, Dellegrottaglie S, Moro C, Lanzillo C, Scatteia A, Di Roma M, Pontone G, Perazzolo Marra M, Barison A, Di Bella G, Cardiac Magnetic Resonance Working Group of the Italian Society of C. Prognostic value of repeating cardiac magnetic resonance in patients with acute myocarditis. *J Am Coll Cardiol* 2019; **74**: 2439–2448.
10. Levick JR, Michel CC. Microvascular fluid exchange and the revised Starling principle. *Cardiovasc Res* 2010; **87**: 198–210.
11. Mehlhorn U, Davis KL, Laine GA, Geissler HJ, Allen SJ. Myocardial fluid balance in acute hypertension. *Microcirculation* 1996; **3**: 371–378.
12. Laine GA. Microvascular changes in the heart during chronic arterial hypertension. *Circ Res* 1988; **62**: 953–960.
13. Nielsen NR, Rangarajan KV, Mao L, Rockman HA, Caron KM. A murine model of increased coronary sinus pressure induces myocardial edema with cardiac lymphatic dilation and fibrosis. *Am J Physiol Heart Circ Physiol* 2020; **318**: H895–H907.
14. Diab OA, Amer MS, Salah El-Din RA. Effect of experimental coronary sinus ligation on myocardial structure and function in the presence or absence of structural heart disease: an insight for the interventional electrophysiologist. *Europace* 2016; **18**: 1897–1904.
15. Davis KL, Laine GA, Geissler HJ, Mehlhorn U, Brennan M, Allen SJ. Effects of myocardial edema on the development of myocardial interstitial fibrosis. *Microcirculation* 2000; **7**: 269–280.
16. Verbrugge FH, Bertrand PB, Willems E, Gielen E, Mullens W, Giri S, Tang WHW, Raman SV, Verhaert D. Global myocardial oedema in advanced decompensated heart failure. *Eur Heart J Cardiovasc Imaging* 2017; **18**: 787–794.
17. Mehlhorn U, Geissler HJ, Laine GA, Allen SJ. Myocardial fluid balance. *Eur J Cardiothorac Surg* 2001; **20**: 1220–1230.
18. Takegawa R, Kabata D, Shimizu K, Hisano S, Ogura H, Shintani A, Shimazu T. Serum albumin as a risk factor for death in patients with prolonged sepsis: an observational study. *J Crit Care* 2019; **51**: 139–144.
19. Boyd JH, Forbes J, Nakada T, Walley KR, Russell JA. Fluid resuscitation in septic shock: A positive fluid balance and elevated central venous pressure are associated with increased mortality. *Crit Care Med* 2011; **39**: 259–265.
20. Pratt JW, Schertel ER, Schaefer SL, Esham KE, McClure DE, Heck CF, Myerowitz PD. Acute transient coronary sinus hypertension impairs left ventricular function and induces myocardial edema. *Am J Physiol* 1996; **271**: H834–H841.
21. Fischer UM, Cox CS, Stewart RH, Laine GA, Allen SJ. Impact of acute myocardial edema on left ventricular function. *J Invest Surg* 2006; **19**: 31–38.
22. Pogátsa G, Dubecz E, Gábor G. The role of myocardial edema in the left ventricular diastolic stiffness. *Basic Res Cardiol* 1976; **71**: 263–269.
23. Scallan J, Huxley VH, Korthuis RJ. *Capillary Fluid Exchange: Regulation, Functions, and Pathology*. San Rafael (CA): Morgan & Claypool Life Sciences; 2010.
24. Lim HS. Cardiogenic shock: failure of oxygen delivery and oxygen utilization. *Clin Cardiol* 2016; **39**: 477–483.
25. Wearn JT. The extent of the capillary bed of the heart. *J Exp Med* 1928; **47**: 273–290.
26. Laughlin MH, Tomanek RJ. Myocardial capillarity and maximal capillary diffusion capacity in exercise-trained dogs. *J Appl Physiol* 1987; **63**: 1481–1486.

27. Feigl EO. Coronary physiology. *Physiol Rev* 1983; **63**: 1–205.
28. Duncker DJ, Bache RJ. Regulation of coronary blood flow during exercise. *Physiol Rev* 2008; **88**: 1009–1086.
29. Bassenge E, Heusch G. Endothelial and neuro-humoral control of coronary blood flow in health and disease. *Rev Physiol Biochem Pharmacol* 1990; **116**: 77–165.
30. Case RB, Felix A, Wachter M, Kyriakidis G, Castellana F. Relative effect of CO2 on canine coronary vascular resistance. *Circ Res* 1978; **42**: 410–418.
31. Grubbström J, Berglund B, Kaijser L. Myocardial blood flow and lactate metabolism at rest and during exercise with reduced arterial oxygen content. *Acta Physiol Scand* 1991; **142**: 467–474.
32. Hiroshi I, Lih K. Acidosis-induced coronary arteriolar dilation is mediated by ATP-sensitive potassium channels in vascular smooth muscle. *Circ Res* 1996; **78**: 50–57.
33. Bünger R, Haddy FJ, Querengässer A, Gerlach E. Studies on potassium induced coronary dilation in the isolated guinea pig heart. *Pflugers Arch* 1976; **363**: 27–31.
34. Mohammed SF, Saad H, Mirzoyev SA, Edwards WD, Maleszewski JJ, Redfield MM. Coronary microvascular rarefaction and myocardial fibrosis in heart failure with preserved ejection fraction. *Circulation* 2015; **131**: 550–559.
35. Schulz R, Janssen F, Guth BD, Heusch G. Effect of coronary hyperperfusion on regional myocardial function and oxygen consumption of stunned myocardium in pigs. *Basic Res Cardiol* 1991; **86**: 534–543.
36. Schulz R, Guth BD, Heusch G. No effect of coronary perfusion on regional myocardial function within the autoregulatory range in pigs. Evidence against the Gregg phenomenon. *Circulation* 1991; **83**: 1390–1403.
37. Westerhof N, Boer C, Lamberts RR, Sipkema P. Cross-talk between cardiac muscle and coronary vasculature. *Physiol Rev* 2006; **86**: 1263–1308.
38. Aldea GS, Mori H, Husseini WK, Austin RE, Hoffman JIE. Effects of increased pressure inside or outside ventricles on total and regional myocardial blood flow. *Am J Physiol Heart Circ Physiol* 2000; **279**: H2927–H2938.
39. Mihailescu LS, Abel FL. Intramyocardial pressure gradients in working and nonworking isolated cat hearts. *Am J Physiol Heart Circ Physiol* 1994; **266**: H1233–H1241.
40. Hoffman JI, Spaan JA. Pressure-flow relations in coronary circulation. *Physiol Rev* 1990; **70**: 331–390.
41. Chilian WM. Microvascular pressures and resistances in the left ventricular subepicardium and subendocardium. *Circ Res* 1991; **69**: 561–570.
42. Merkus D, Vergroesen I, Hiramatsu O, Tachibana H, Nakamoto H, Toyota E, Goto M, Ogasawara Y, Spaan JAE, Kajiya F. Stenosis differentially affects subendocardial and subepicardial arterioles in vivo. *Am J Physiol Heart Circ Physiol* 2001; **280**: H1674–H1682.
43. Heusch G. Myocardial ischemia: lack of coronary blood flow, myocardial oxygen supply-demand imbalance, or what? *Am J Physiol Heart Circ Physiol* 2019; **316**: H1439–H1446.
44. Levy BI, Heusch G, Camici PG. The many faces of myocardial ischaemia and angina. *Cardiovasc Res* 2019; **115**: 1460–1470.
45. Luetkens JA, Isaak A, Öztürk C, Mesropyan N, Monin M, Schlabe S, Reinert M, Faron A, Heine A, Velten M, Dabir D, Boesecke C, Strassburg CP, Attenberger U, Zimmer S, Duerr GD, Nattermann J. Cardiac MRI in suspected acute COVID-19 myocarditis. *Radiol: Cardiothoracic Imaging* 2021; **3**: e200628.
46. Vasques-Nóvoa F, Laundos TL, Madureira A, Bettencourt N, Nunes JPL, Carneiro F, Paiva JA, Pinto-do-Ó P, Nascimento DS, Leite-Moreira AF, Roncon-Albuquerque R. Myocardial Edema: an Overlooked Mechanism of Septic Cardiomyopathy? *Shock* 2020; **53**: 616–619.
47. Vasques-Novoa F, Angelico-Goncalves A, Bettencourt N, Leite-Moreira AF, Roncon-Albuquerque R. Myocardial edema and remodeling: a link between acute myocarditis and septic cardiomyopathy? *J Am Coll Cardiol* 2020; **75**: 1497–1498.
48. McCulloch AD, Hunter PJ, Smaill BH. Mechanical effects of coronary perfusion in the passive canine left ventricle. *Am J Physiol Heart Circ Physiol* 1992; **262**: H523–H530.
49. Gaasch WH, Bernard SA. The effect of acute changes in coronary blood flow on left ventricular end-diastolic wall thickness. An echocardiographic study. *Circulation* 1977; **56**: 593–598.
50. Allaart CP, Sipkema P, Westerhof N. Effect of perfusion pressure on diastolic stress-strain relations of isolated rat papillary muscle. *Am J Physiol Heart Circ Physiol* 1995; **268**: H945–H954.
51. Goto Y, Slinker BK, LeWinter MM. Effect of coronary hyperemia on Emax and oxygen consumption in blood-perfused rabbit hearts. Energetic consequences of Gregg's phenomenon. *Circ Res* 1991; **68**: 482–492.
52. Watanabe J, Levine MJ, Bellotto F, Johnson RG, Grossman W. Effects of coronary venous pressure on left ventricular diastolic distensibility. *Circ Res* 1990; **67**: 923–932.
53. Charan NB, Ripley R, Carvalho P. Effect of increased coronary venous pressure on left ventricular function in sheep. *Respir Physiol* 1998; **112**: 227–235.
54. Ilbawi MN, Idriss FS, Muster AJ, DeLeon SY, Berry TE, Duffy CE, Paul MH. Effects of elevated coronary sinus pressure on left ventricular function after the Fontan operation. An experimental and clinical correlation. *J Thorac Cardiovasc Surg* 1986; **92**: 231–237.
55. Rahimi N. Defenders and challengers of endothelial barrier function. *Front Immunol* 2017; **8**: 1847.
56. Sidibé A, Imhof BA. VE-cadherin phosphorylation decides: vascular permeability or diapedesis. *Nat Immunol* 2014; **15**: 215–217.
57. Dejana E, Orsenigo F, Lampugnani MG. The role of adherens junctions and VE-cadherin in the control of vascular permeability. *J Cell Sci* 2008; **121**: 2115–2122.
58. Swager SA, Delfín DA, Rastogi N, Wang H, Canan BD, Fedorov VV, Mohler PJ, Kilic A, Higgins RSD, Ziolo MT, Janssen PML, Rafael-Fortney JA. Claudin-5 levels are reduced from multiple cell types in human failing hearts and are associated with mislocalization of ephrin-B1. *Cardiovasc Pathol* 2015; **24**: 160–167.
59. Jia G, Habibi J, Aroor AR, Hill MA, DeMarco VG, Lee LE, Ma L, Barron BJ, Whaley-Connell A, Sowers JR. Enhanced endothelium epithelial sodium channel signaling prompts left ventricular diastolic dysfunction in obese female mice. *Metab Clin Exp* 2018; **78**: 69–79.
60. Schäfer R, Abraham D, Paulus P, Blumer R, Grimm M, Wojta J, Aharinejad S. Impaired VE-cadherin/beta-catenin expression mediates endothelial cell degeneration in dilated cardiomyopathy. *Circulation* 2003; **108**: 1585–1591.
61. Weis S, Shintani S, Weber A, Kirchmair R, Wood M, Cravens A, McSharry H, Iwakura A, Yoon YS, Himes N, Burstein D, Doukas J, Soll R, Losordo D, Cheresh D. Src blockade stabilizes a Flk/cadherin complex, reducing edema and tissue injury following myocardial infarction. *J Clin Invest* 2004; **113**: 885–894.
62. Giacomelli F, Anversa P, Wiener J. Effect of angiotensin-induced hypertension on rat coronary arteries and myocardium. *Am J Pathol* 1976; **84**: 111–138.
63. Castanares-Zapatero D, Bouleti C, Sommereyns C, Gerber B, Lecut C, Mathivet T, Horckmans M, Communi D, Foretz M, Vanoverschelde J-L, Germain S, Bertrand L, Laterre P-F, Oury C, Viollet B, Horman S, Beauloye C. Connection Between Cardiac Vascular Permeability, Myocardial Edema, and Inflammation During Sepsis. *Crit Care Med* 2013; **41**: e411–e422.
64. Vasques-Nóvoa F, Laundos TL, Cerqueira RJ, Quina-Rodrigues C, Soares-Dos-Reis R, Baganha F, Ribeiro S, Mendonça L, Gonçalves F, Reguenga C, Verhesen W, Carneiro F, Paiva JA, Schroen B, Castro-Chaves P, Pinto-do-Ó P, Nascimento DS, Heymans S, Leite-Moreira AF, Roncon-Albuquerque

R. MicroRNA-155 amplifies nitric oxide/cGMP signaling and impairs vascular angiotensin II reactivity in septic shock. *Crit Care Med* 2018; **46**: e945–e954.
65. Jenkins EL, Caputo M, Angelini GD, Ghorbel MT. Chronic hypoxia down-regulates tight junction protein ZO-2 expression in children with cyanotic congenital heart defect. *ESC Heart Fail* 2016; **3**: 131–137.
66. Khan TA, Bianchi C, Araujo E, Voisine P, Xu S-H, Feng J, Li J, Sellke FW. Aprotinin preserves cellular junctions and reduces myocardial edema after regional ischemia and cardioplegic arrest. *Circulation* 2005; **112**: I196–I201.
67. Haidari M, Zhang W, Willerson JT, Dixon RA. Disruption of endothelial adherens junctions by high glucose is mediated by protein kinase C-β-dependent vascular endothelial cadherin tyrosine phosphorylation. *Cardiovasc Diabetol* 2014; **13**: 105.
68. Rao R. Oxidative stress-induced disruption of epithelial and endothelial tight junctions. *Front Biosci* 2008; **13**: 7210–7226.
69. Magalhaes A, Matias I, Palmela I, Brito MA, Dias S. LDL-cholesterol increases the transcytosis of molecules through endothelial monolayers. *PLoS ONE* 2016; **11**: e0163988.
70. Mani AM, Chattopadhyay R, Singh NK, Rao GN. Cholesterol crystals increase vascular permeability by inactivating SHP2 and disrupting adherens junctions. *Free Radic Biol Med* 2018; **123**: 72–84.
71. Wang L, Chen Y, Li X, Zhang Y, Gulbins E, Zhang Y. Enhancement of endothelial permeability by free fatty acid through lysosomal cathepsin B-mediated Nlrp3 inflammasome activation. *Oncotarget* 2016; **7**: 73229–73241.
72. Becker BF, Chappell D, Jacob M. Endothelial glycocalyx and coronary vascular permeability: the fringe benefit. *Basic Res Cardiol* 2010; **105**: 687–701.
73. Becker BF, Jacob M, Leipert S, Salmon AHJ, Chappell D. Degradation of the endothelial glycocalyx in clinical settings: searching for the sheddases. *Br J Clin Pharmacol* 2015; **80**: 389–402.
74. Jedlicka J, Becker BF, Chappell D. Endothelial glycocalyx. *Crit Care Clin* 2020; **36**: 217–232.
75. Gandhi NS, Mancera RL. The structure of glycosaminoglycans and their interactions with proteins. *Chem Biol Drug Des* 2008; **72**: 455–482.
76. Kolářová H, Ambrůzová B, Švihálková Šindlerová L, Klinke A, Kubala L. Modulation of endothelial glycocalyx structure under inflammatory conditions. *Mediators Inflamm* 2014; **2014**: 1–17.
77. Reitsma S, Slaaf DW, Vink H, van Zandvoort MA, ouder Egbrink MG. The endothelial glycocalyx: composition, functions, and visualization. *Pflugers Arch* 2007; **454**: 345–359.
78. Annecke T, Chappell D, Chen C, Jacob M, Welsch U, Sommerhoff CP, Rehm M, Conzen PF, Becker BF. Sevoflurane preserves the endothelial glycocalyx against ischaemia-reperfusion injury. *Br J Anaesth* 2010; **104**: 414–421.
79. Ward BJ, Donnelly JL. Hypoxia induced disruption of the cardiac endothelial glycocalyx: implications for capillary permeability. *Cardiovasc Res* 1993; **27**: 384–389.
80. Diebel LN, Diebel ME, Martin JV, Liberati DM. Acute hyperglycemia exacerbates trauma-induced endothelial and glycocalyx injury: an in vitro model. *J Trauma Acute Care Surg* 2018; **85**: 960–967.
81. Huebener P, Abou-Khamis T, Zymek P, Bujak M, Ying X, Chatila K, Haudek S, Thakker G, Frangogiannis NG. CD44 is critically involved in infarct healing by regulating the inflammatory and fibrotic response. *J Immunol* 2008; **180**: 2625–2633.
82. Vanhoutte D, Schellings MWM, Götte M, Swinnen M, Herias V, Wild MK, Vestweber D, Chorianopoulos E, Cortés V, Rigotti A, Stepp M-A, Van de Werf F, Carmeliet P, Pinto YM, Heymans S. Increased expression of syndecan-1 protects against cardiac dilatation and dysfunction after myocardial infarction. *Circulation* 2007; **115**: 475–482.
83. Rienks M, Carai P, van Teeffelen J, Eskens B, Verhesen W, Hemmeryckx B, Johnson DM, van Leeuwen R, Jones EA, Heymans S, Papageorgiou A-P. SPARC preserves endothelial glycocalyx integrity, and protects against adverse cardiac inflammation and injury during viral myocarditis. *Matrix Biol* 2018; **74**: 21–34.
84. Gotloib L, Shostak A, Galdi P, Jaichenko J, Fudin R. Loss of microvascular negative charges accompanied by interstitial edema in septic rats' heart. *Circ Shock* 1992; **36**: 45–56.
85. Wiesinger A, Peters W, Chappell D, Kentrup D, Reuter S, Pavenstädt H, Oberleithner H, Kümpers P. Nanomechanics of the Endothelial Glycocalyx in Experimental Sepsis. *PLoS ONE* 2013; **8**: e80905.
86. van den Berg BM, Vink H, Spaan JA. The endothelial glycocalyx protects against myocardial edema. *Circ Res* 2003; **92**: 592–594.
87. Bruegger D, Rehm M, Jacob M, Chappell D, Stoeckelhuber M, Welsch U, Conzen P, Becker BF. Exogenous nitric oxide requires an endothelial glycocalyx to prevent postischemic coronary vascular leak in guinea pig hearts. *Crit Care* 2008; **12**: R73.
88. Bruegger D, Jacob M, Rehm M, Loetsch M, Welsch U, Conzen P, Becker BF. Atrial natriuretic peptide induces shedding of endothelial glycocalyx in coronary vascular bed of guinea pig hearts. *Am J Physiol Heart Circ Physiol* 2005; **289**: H1993–H1999.
89. Chappell D, Bruegger D, Potzel J, Jacob M, Brettner F, Vogeser M, Conzen P, Becker BF, Rehm M. Hypervolemia increases release of atrial natriuretic peptide and shedding of the endothelial glycocalyx. *Crit Care* 2014; **18**: 538.
90. Curry FRE. Atrial natriuretic peptide: an essential physiological regulator of transvascular fluid, protein transport, and plasma volume. *J Clin Invest* 2005; **115**: 1458–1461.
91. Huxley VH, Tucker VL, Verburg KM, Freeman RH. Increased capillary hydraulic conductivity induced by atrial natriuretic peptide. *Circ Res* 1987; **60**: 304–307.
92. Jacob M, Saller T, Chappell D, Rehm M, Welsch U, Becker BF. Physiological levels of A-, B- and C-type natriuretic peptide shed the endothelial glycocalyx and enhance vascular permeability. *Basic Res Cardiol* 2013; **108**: 347.
93. Oberleithner H, Peters W, Kusche-Vihrog K, Korte S, Schillers H, Kliche K, Oberleithner K. Salt overload damages the glycocalyx sodium barrier of vascular endothelium. *Pflugers Arch* 2011; **462**: 519–528.
94. Nijst P, Verbrugge FH, Grieten L, Dupont M, Steels P, Tang WHW, Mullens W. The pathophysiological role of interstitial sodium in heart failure. *J Am Coll Cardiol* 2015; **65**: 378–388.
95. Bode L, Eklund EA, Murch S, Freeze HH. Heparan sulfate depletion amplifies TNF-α-induced protein leakage in an in vitro model of protein-losing enteropathy. *Am J Physiol Gastrointest Liver Physiol* 2005; **288**: G1015–G1023.
96. Oberleithner H, Riethmüller C, Schillers H, MacGregor GA, de Wardener HE, Hausberg M. Plasma sodium stiffens vascular endothelium and reduces nitric oxide release. *Proc Natl Acad Sci U S A* 2007; **104**: 16281–16286.
97. Chelazzi C, Villa G, Mancinelli P, De Gaudio AR, Adembri C. Glycocalyx and sepsis-induced alterations in vascular permeability. *Crit Care* 2015; **19**: 26.
98. Uchimido R, Schmidt EP, Shapiro NI. The glycocalyx: a novel diagnostic and therapeutic target in sepsis. *Crit Care* 2019; **23**: 16.
99. Armulik A, Genové G, Betsholtz C. Pericytes: Developmental, Physiological, and Pathological Perspectives, Problems, and Promises. *Dev Cell* 2011; **21**: 193–215.
100. Lee LL, Chintalgattu V. Pericytes in the heart. *Adv Exp Med Biol* 2019; **1122**: 187–210.
101. Nees S, Weiss DR, Senftl A, Knott M, Forch S, Schnurr M, Weyrich P, Juchem G. Isolation, bulk cultivation, and characterization of coronary microvascular pericytes: the second most frequent myocardial cell type in vitro. *Am J Physiol Heart Circ Physiol* 2012; **302**: H69–H84.

102. Annika A, Alexandra A, Christer B. Endothelial/Pericyte interactions. *Circ Res* 2005; **97**: 512–523.
103. Avolio E, Madeddu P. Discovering cardiac pericyte biology: from physiopathological mechanisms to potential therapeutic applications in ischemic heart disease. *Vascul Pharmacol* 2016; **86**: 53–63.
104. Ziegler T, Horstkotte J, Schwab C, Pfetsch V, Weinmann K, Dietzel S, Rohwedder I, Hinkel R, Gross L, Lee S, Hu J, Soehnlein O, Franz WM, Sperandio M, Pohl U, Thomas M, Weber C, Augustin HG, Fassler R, Deutsch U, Kupatt C. Angiopoietin 2 mediates microvascular and hemodynamic alterations in sepsis. *J Clin Invest* 2013; **123**: 3436–3445.
105. Chintalgattu V, Rees ML, Culver JC, Goel A, Jiffar T, Zhang J, Dunner K, Pati S, Bankson JA, Pasqualini R, Arap W, Bryan NS, Taegtmeyer H, Langley RR, Yao H, Kupferman ME, Entman ML, Dickinson ME, Khakoo AY. Coronary microvascular pericytes are the cellular target of sunitinib malate-induced cardiotoxicity. *Sci Transl Med* 2013; **5**: 187ra69.
106. Zeng H, He X, Tuo QH, Liao DF, Zhang GQ, Chen JX. LPS causes pericyte loss and microvascular dysfunction via disruption of Sirt3/angiopoietins/Tie-2 and HIF-2alpha/Notch3 pathways. *Sci Rep* 2016; **6**: 20931.
107. He X, Zeng H, Chen J-X. Ablation of SIRT3 causes coronary microvascular dysfunction and impairs cardiac recovery post myocardial ischemia. *Int J Cardiol* 2016; **215**: 349–357.
108. Tao Y-K, Zeng H, Zhang G-Q, Chen ST, Xie X-J, He X, Wang S, Wen H, Chen J-X. Notch3 deficiency impairs coronary microvascular maturation and reduces cardiac recovery after myocardial ischemia. *Int J Cardiol* 2017; **236**: 413–422.
109. Zeng H, Vaka VR, He X, Booz GW, Chen J-X. High-fat diet induces cardiac remodelling and dysfunction: assessment of the role played by SIRT3 loss. *J Cell Mol Med* 2015; **19**: 1847–1856.
110. Siao C-J, Lorentz CU, Kermani P, Marinic T, Carter J, McGrath K, Padow VA, Mark W, Falcone DJ, Cohen-Gould L, Parrish DC, Habecker BA, Nykjaer A, Ellenson LH, Tessarollo L, Hempstead BL. ProNGF, a cytokine induced after myocardial infarction in humans, targets pericytes to promote microvascular damage and activation. *J Exp Med* 2012; **209**: 2291–2305.
111. Bischoff FC, Werner A, John D, Boeckel J-N, Melissari M-T, Grote P, Glaser SF, Demolli S, Uchida S, Michalik KM, Meder B, Katus HA, Haas J, Chen W, Pullamsetti SS, Seeger W, Zeiher AM, Dimmeler S, Zehendner CM. Identification and Functional Characterization of Hypoxia-Induced Endoplasmic Reticulum Stress Regulating lncRNA (HypERlnc) in Pericytes. *Circ Res* 2017; **121**: 368–375.
112. O'Farrell FM, Mastitskaya S, Hammond-Haley M, Freitas F, Wah WR, Attwell D. Capillary pericytes mediate coronary no-reflow after myocardial ischaemia. *Elife* 2017; **6**: e29280.
113. Grant RI, Hartmann DA, Underly RG, Berthiaume A-A, Bhat NR, Shih AY. Organizational hierarchy and structural diversity of microvascular pericytes in adult mouse cortex. *J Cereb Blood Flow Metab* 2019; **39**: 411–425.
114. Peppiatt CM, Howarth C, Mobbs P, Attwell D. Bidirectional control of CNS capillary diameter by pericytes. *Nature* 2006; **443**: 700–704.
115. Greenhalgh SN, Iredale JP, Henderson NC. Origins of fibrosis: pericytes take centre stage. *F1000Prime Rep* 2013; **5**: 37.
116. Schrimpf C, Duffield JS. Mechanisms of fibrosis: the role of the pericyte. *Curr Opin Nephrol Hypertens* 2011; **20**: 297–305.
117. Suthahar N, Meijers WC, Silljé HHW, Ho JE, Liu F-T, de Boer RA. Galectin-3 activation and inhibition in heart failure and cardiovascular disease: an update. *Theranostics* 2018; **8**: 593–609.
118. McCullough PA, Olobatoke A, Vanhecke TE. Galectin-3: a novel blood test for the evaluation and management of patients with heart failure. *Rev Cardiovasc Med* 2011; **12**: 200–210.
119. Kramann R, Schneider RK, DiRocco DP, Machado F, Fleig S, Bondzie PA, Henderson JM, Ebert BL, Humphreys BD. Perivascular Gli1+ progenitors are key contributors to injury-induced organ fibrosis. *Cell Stem Cell* 2015; **16**: 51–66.
120. van Dijk CGM, Oosterhuis NR, Xu YJ, Brandt M, Paulus WJ, van Heerebeek L, Duncker DJ, Verhaar MC, Fontoura D, Lourenço AP, Leite-Moreira AF, Falcão-Pires I, Joles JA, Cheng C. Distinct endothelial cell responses in the heart and kidney microvasculature characterize the progression of heart failure with preserved ejection fraction in the obese ZSF1 rat with cardiorenal metabolic syndrome. *Circ Heart Fail* 2016; **9**: e002760.
121. Guijarro-Munoz I, Compte M, Alvarez-Cienfuegos A, Alvarez-Vallina L, Sanz L. Lipopolysaccharide activates Toll-like receptor 4 (TLR4)-mediated NF-kappaB signaling pathway and proinflammatory response in human pericytes. *J Biol Chem* 2014; **289**: 2457–2468.
122. Rudziak P, Ellis CG, Kowalewska PM. Role and molecular mechanisms of pericytes in regulation of leukocyte diapedesis in inflamed tissues. *Mediators Inflamm* 2019; **2019**: 4123605.
123. Eckhouse SR, Spinale FG. Changes in the myocardial interstitium and contribution to the progression of heart failure. *Heart Fail Clin* 2012; **8**: 7–20.
124. Beyar R, Ben-Ari R, Gibbons-Kroeker CA, Tyberg JV, Sideman S. Effect of interconnecting collagen fibres on left ventricular function and intramyocardial compression. *Cardiovasc Res* 1993; **27**: 2254–2263.
125. Pine MB, Brooks WW, Nosta JJ, Abelmann WH. Hydrostatic forces limit swelling of rat ventricular myocardium. *Am J Physiol Heart Circ Physiol* 1981; **241**: H740–H747.
126. Lamberts RR, Willemsen MJJMF, Pérez NG, Sipkema P, Westerhof N. Acute and specific collagen type I degradation increases diastolic and developed tension in perfused rat papillary muscle. *Am J Physiol Heart Circ Physiol* 2004; **286**: H889–H894.
127. Baicu CF, Stroud JD, Livesay VA, Hapke E, Holder J, Spinale FG, Zile MR. Changes in extracellular collagen matrix alter myocardial systolic performance. *Am J Physiol Heart Circ Physiol* 2003; **284**: H122–H132.
128. Sorokin L. The impact of the extracellular matrix on inflammation. *Nat Rev Immunol* 2010; **10**: 712–723.
129. Li J, Schwimmbeck PL, Tschope C, Leschka S, Husmann L, Rutschow S, Reichenbach F, Noutsias M, Kobalz U, Poller W, Spillmann F, Zeichhardt H, Schultheiss H-P, Pauschinger M. Collagen degradation in a murine myocarditis model: relevance of matrix metalloproteinase in association with inflammatory induction. *Cardiovasc Res* 2002; **56**: 235–247.
130. Yu P, Boughner DR, Sibbald WJ, Keys J, Dunmore J, Martin CM. Myocardial collagen changes and edema in rats with hyperdynamic sepsis. *Crit Care Med* 1997; **25**: 657–662.
131. Azevedo PS, Polegato BF, Minicucci MF, Paiva SAR, Zornoff LAM. Cardiac remodeling: concepts, clinical impact, pathophysiological mechanisms and pharmacologic treatment. *Arq Bras Cardiol* 2016; **106**: 62–69.
132. Jiang D, Liang J, Noble PW. Hyaluronan in tissue injury and repair. *Annu Rev Cell Dev Biol* 2007; **23**: 435–461.
133. Dogné S, Rath G, Jouret F, Caron N, Dessy C, Flamion B. Hyaluronidase 1 deficiency preserves endothelial function and glycocalyx integrity in early streptozotocin-induced diabetes. *Diabetes* 2016; **65**: 2742–2753.
134. Chowdhury B, Hemming R, Hombach-Klonisch S, Flamion B, Triggs-Raine B. Murine hyaluronidase 2 deficiency results in extracellular hyaluronan accumulation and severe cardiopulmonary dysfunction. *J Biol Chem* 2013; **288**: 520–528.
135. Waldenstrom A, Martinussen HJ, Gerdin B, Hallgren R. Accumulation of hyaluronan and tissue edema in experimental myocardial infarction. *J Clin Invest* 1991; **88**: 1622–1628.
136. Lorén CE, Dahl CP, Do L, Almaas VM, Geiran OR, Mörner S, Hellman U. Low molecular mass myocardial hyaluronan in human hypertrophic cardiomyopathy. *Cell* 2019; **8**: 97.

137. Waldenström A, Fohlman J, Ilbäcky NG, Ronquist G, Hällgren R, Gerdin B. Coxsackie B3 myocarditis induces a decrease in energy charge and accumulation of hyaluronan in the mouse heart. *Eur J Clin Invest* 1993; **23**: 277–282.
138. Johnsson C, Tufveson G, Hällgren R, Elvin A, Gerdin B. Hyaluronidase ameliorates rejection-induced edema. *Transpl Int* 1999; **12**: 235–243.
139. Johnsson C, Hallgren R, Tufveson G. Hyaluronidase can be used to reduce interstitial edema in the presence of heparin. *J Cardiovasc Pharmacol Ther* 2000; **5**: 229–236.
140. Cuijpers I, Simmonds SJ, van Bilsen M, Czarnowska E, González Miqueo A, Heymans S, Kuhn AR, Mulder P, Ratajska A, Jones EAV, Brakenhielm E. Microvascular and lymphatic dysfunction in HFpEF and its associated comorbidities. *Basic Res Cardiol* 2020; **115**: 39.
141. Jackson DG. Leucocyte trafficking via the lymphatic vasculature—mechanisms and consequences. *Front Immunol* 2019; **10**: 471.
142. Schwager S, Detmar M. Inflammation and lymphatic function. *Front Immunol* 2019; **10**: 308.
143. Leak LV, Burke JF. Ultrastructural studies on the lymphatic anchoring filaments. *J Cell Biol* 1968; **36**: 129–149.
144. Klaourakis K, Vieira JM, Riley PR. The evolving cardiac lymphatic vasculature in development, repair and regeneration. *Nat Rev Cardiol* 2021; **18**: 368–379.
145. Leak LV. The structure of lymphatic capillaries in lymph formation. *Fed Proc* 1976; **35**: 1863–1871.
146. Brakenhielm E, Alitalo K. Cardiac lymphatics in health and disease. *Nat Rev Cardiol* 2019; **16**: 56–68.
147. Aspelund A, Robciuc MR, Karaman S, Makinen T, Alitalo K. Lymphatic system in cardiovascular medicine. *Circ Res* 2016; **118**: 515–530.
148. Dongaonkar RM, Stewart RH, Quick CM, Uray KL, Cox CS, Laine GA. AWARD ARTICLE: Microcirculatory Society Award for Excellence in Lymphatic ResearchTime Course of Myocardial Interstitial Edema Resolution and Associated Left Ventricular Dysfunction. *Microcirculation* 2012; **19**: 714–722.
149. Vieira JM, Norman S, Villa del Campo C, Cahill TJ, Barnette DN, Gunadasa-Rohling M, Johnson LA, Greaves DR, Carr CA, Jackson DG, Riley PR. The cardiac lymphatic system stimulates resolution of inflammation following myocardial infarction. *J Clin Invest* 2020; **128**: 3402–3412.
150. Al-Kofahi M, Omura S, Tsunoda I, Sato F, Becker F, Gavins FNE, Woolard MD, Pattillo C, Zawieja D, Muthuchamy M, Gashev A, Shihab I, Ghoweba M, Von der Weid P-Y, Wang Y, Alexander JS. IL-1β reduces cardiac lymphatic muscle contraction via COX-2 and PGE2 induction: potential role in myocarditis. *Biomed Pharmacother* 2018; **107**: 1591–1600.
151. Tan KW, Chong SZ, Wong FHS, Evrard M, Tan SM-L, Keeble J, Kemeny DM, Ng LG, Abastado J-P, Angeli V. Neutrophils contribute to inflammatory lymphangiogenesis by increasing VEGF-A bioavailability and secreting VEGF-D. *Blood* 2013; **122**: 3666–3677.
152. Mahmoud Houssari, Anais Dumesnil, Virginie Tardif, Riikka Kivelä, Nathalie Pizzinat, Ines Boukhalfa, David Godefroy, Damien Schapman, Hemanthakumar Karthik A., Mathilde Bizou, Jean-Paul Henry, Sylvanie Renet, Gaetan Riou, Julie Rondeaux, Youssef Anouar, Sahil Adriouch, Sylvain Fraineau, Kari Alitalo, Vincent Richard, Paul Mulder, Ebba Brakenhielm, eds. Lymphatic and immune cell cross-talk regulates cardiac recovery after experimental myocardial infarction. *Arterioscler Thromb Vasc Biol* 2020; **40**: 1722–1737.
153. Henri O, Pouehe C, Houssari M, Galas L, Nicol L, Edwards-Levy F, Henry JP, Dumesnil A, Boukhalfa I, Banquet S, Schapman D, Thuillez C, Richard V, Mulder P, Brakenhielm E. Selective stimulation of cardiac lymphangiogenesis reduces myocardial edema and fibrosis leading to improved cardiac function following myocardial infarction. *Circulation* 2016; **133**: 1484–1497 discussion 1497.
154. Trincot CE, Xu W, Zhang H, Kulikauskas MR, Caranasos TG, Jensen BC, Sabine A, Petrova TV, Caron KM. Adrenomedullin induces cardiac lymphangiogenesis after myocardial infarction and regulates cardiac edema via Connexin 43. *Circ Res* 2019; **124**: 101–113.
155. Shimizu Y, Polavarapu R, Eskla K-L, Pantner Y, Nicholson CK, Ishii M, Brunnhoelzl D, Mauria R, Husain A, Naqvi N, Murohara T, Calvert JW. Impact of lymphangiogenesis on cardiac remodeling after ischemia and reperfusion injury. *J Am Heart Assoc* 2018; **7**: e009565.
156. Zhang H-F, Wang Y-L, Tan Y-Z, Wang H-J, Tao P, Zhou P. Enhancement of cardiac lymphangiogenesis by transplantation of CD34+VEGFR-3+ endothelial progenitor cells and sustained release of VEGF-C. *Basic Res Cardiol* 2019; **114**: 43.
157. Keller TCS, Lim L, Shewale SV, McDaid K, Martí-Pàmies Í, Tang AT, Wittig C, Guerrero AA, Sterling S, Leu NA, Scherrer-Crosbie M, Gimotty PA, Kahn ML. Genetic blockade of lymphangiogenesis does not impair cardiac function after myocardial infarction. *J Clin Invest* 2021; **131**: 1–10.
158. Hoffmann EK, Lambert IH, Pedersen SF. Physiology of cell volume regulation in vertebrates. *Physiol Rev* 2009; **89**: 193–277.
159. Gonano LA, Morell M, Burgos JI, Dulce RA, De Giusti VC, Aiello EA, Hare JM, Vila Petroff M. Hypotonic swelling promotes nitric oxide release in cardiac ventricular myocytes: impact on swelling-induced negative inotropic effect. *Cardiovasc Res* 2014; **104**: 456–466.
160. Lang F, Busch GL, Ritter M, Völkl H, Waldegger S, Gulbins E, Häussinger D. Functional significance of cell volume regulatory mechanisms. *Physiol Rev* 1998; **78**: 247–306.
161. Lang F. Mechanisms and significance of cell volume regulation. *J Am Coll Nutr* 2007; **26**: 613S–623S.
162. Garcia-Dorado D, Theroux P, Munoz R, Alonso J, Elizaga J, Fernandez-Aviles F, Botas J, Solares J, Soriano J, Duran JM. Favorable effects of hyperosmotic reperfusion on myocardial edema and infarct size. *Am J Physiol Heart Circ Physiol* 1992; **262**: H17–H22.
163. Heusch G. Treatment of myocardial ischemia/reperfusion injury by ischemic and pharmacological postconditioning. *Compr Physiol* 2015: 1123–1145.
164. Zhao M. Increase in myofilament separation in the "stunned" myocardium. *J Mol Cell Cardiol* 1992; **24**: 269–276.
165. Ferreira VM, Schulz-Menger J, Holmvang G, Kramer CM, Carbone I, Sechtem U, Kindermann I, Gutberlet M, Cooper LT, Liu P, Friedrich MG. Cardiovascular magnetic resonance in nonischemic myocardial inflammation. *J Am Coll Cardiol* 2018; **72**: 3158–3176.
166. Fernandez-Jimenez R, Garcia-Prieto J, Sanchez-Gonzalez J, Aguero J, Lopez-Martin GJ, Galan-Arriola C, Molina-Iracheta A, Doohan R, Fuster V, Ibanez B. Pathophysiology underlying the bimodal edema phenomenon after myocardial ischemia/reperfusion. *J Am Coll Cardiol* 2015; **66**: 816–828.
167. Fernández-Jiménez R, Barreiro-Pérez M, Martin-García A, Sánchez-González J, Agüero J, Galán-Arriola C, García-Prieto J, Díaz-Pelaez E, Vara P, Martinez I, Zamarro I, Garde B, Sanz J, Fuster V, Sánchez PL, Ibanez B. Dynamic Edematous Response of the Human Heart to Myocardial Infarction. *Circulation* 2017; **136**: 1288–1300.
168. Hausenloy DJ, Chilian W, Crea F, Davidson SM, Ferdinandy P, Garcia-Dorado D, van Royen N, Schulz R, Heusch G. The coronary circulation in acute myocardial ischaemia/reperfusion injury: a target for cardioprotection. *Cardiovasc Res* 2019; **115**: 1143–1155.
169. Díaz-Munoz R, Valle-Caballero MJ, Sanchez-Gonzalez J, Pizarro G, García-Rubira JC, Escalera N, Fuster V, Fernández-Jiménez R, Ibanez B. Intravenous metoprolol during ongoing STEMI ameliorates markers of ischemic injury: a METOCARD-CNIC trial electrocardiographic study. *Basic Res Cardiol* 2021; **116**: 45.

170. Heusch G. Myocardial ischaemia-reperfusion injury and cardioprotection in perspective. *Nat Rev Cardiol* 2020; **17**: 773–789.
171. Heusch G. Myocardial stunning and hibernation revisited. *Nat Rev Cardiol* 2021; **18**: 522–536.
172. Heusch G. Coronary microvascular obstruction: the new frontier in cardioprotection. *Basic Res Cardiol* 2019; **114**: 45.
173. Manciet LH, Poole DC, McDonagh PF, Copeland JG, Mathieu-Costello O. Microvascular compression during myocardial ischemia: mechanistic basis for no-reflow phenomenon. *Am J Physiol Heart Circ Physiol* 1994; **266**: H1541–H1550.
174. Heusch P, Nensa F, Heusch G. Is MRI really the gold standard for the quantification of salvage from myocardial infarction? *Circ Res* 2015; **117**: 222–224.
175. Zia MI, Ghugre NR, Connelly KA, Strauss BH, Dick AJ, Wright G. Diabetes is associated with increased and persistent myocardial edema in infarct segment post acute myocardial infarction. *J Cardiovasc Magn Reson* 2012; **14**: P29.
176. Zia MI, Ghugre NR, Roifman I, Strauss BH, Walcarius R, Mohammed M, Sparkes JD, Dick AJ, Wright GA, Connelly KA. Comparison of the frequencies of myocardial edema determined by cardiac magnetic resonance in diabetic versus nondiabetic patients having percutaneous coronary intervention for ST elevation myocardial infarction. *Am J Cardiol* 2014; **113**: 607–612.
177. Alvarado T, Cecconi A, Antuna P, Salamanca J, Nogales-Romo MT, Viliani D, Pozo E, Diego G, Rojas-Gonzalez A, Rivero F, Hernandez Muniz S, Olivera MJ, Caballero P, Jimenez-Borreguero J, Alfonso F. Diabetes paradox in Tako-Tsubo cardiomyopathy: beneficial effect of diabetes on myocardial edema. *Eur Heart J* 2018; **39**: ehy563-P4394.
178. Cooper S, Teoh H, Campeau MA, Verma S, Leask RL. Empagliflozin restores the integrity of the endothelial glycocalyx in vitro. *Mol Cell Biochem* 2019; **459**: 121–130.
179. Anker SD, Butler J, Filippatos G, Ferreira JP, Bocchi E, Böhm M, Brunner-La Rocca H-P, Choi D-J, Chopra V, Chuquiure-Valenzuela E, Giannetti N, Gomez-Mesa JE, Janssens S, Januzzi JL, Gonzalez-Juanatey JR, Merkely B, Nicholls SJ, Perrone SV, Piña IL, Ponikowski P, Senni M, Sim D, Spinar J, Squire I, Taddei S, Tsutsui H, Verma S, Vinereanu D, Zhang J, Carson P, Lam CSP, Marx N, Zeller C, Sattar N, Jamal W, Schnaidt S, Schnee JM, Brueckmann M, Pocock SJ, Zannad F, Packer M, EMPEROR-Preserved Trial Investigators. Empagliflozin in heart failure with a preserved ejection fraction. *N Engl J Med* 2021; **385**: 1451–1461.
180. Packer M, Anker SD, Butler J, Filippatos G, Pocock SJ, Carson P, Januzzi J, Verma S, Tsutsui H, Brueckmann M, Jamal W, Kimura K, Schnee J, Zeller C, Cotton D, Bocchi E, Böhm M, Choi D-J, Chopra V, Chuquiure E, Giannetti N, Janssens S, Zhang J, Gonzalez Juanatey JR, Kaul S, Brunner-La Rocca H-P, Merkely B, Nicholls SJ, Perrone S, Pina I, Ponikowski P, Sattar N, Senni M, Seronde MF, Spinar J, Squire I, Taddei S, Wanner C, Zannad F, EMPEROR-Reduced Trial Investigators. Cardiovascular and renal outcomes with empagliflozin in heart failure. *N Engl J Med* 2020; **383**: 1413–1424.
181. Pitt B, Zannad F, Remme WJ, Cody R, Castaigne A, Perez A, Palensky J, Wittes J. The effect of spironolactone on morbidity and mortality in patients with severe heart failure. *N Engl J Med* 1999; **341**: 709–717.
182. Pitt B, Pfeffer MA, Assmann SF, Boineau R, Anand IS, Claggett B, Clausell N, Desai AS, Diaz R, Fleg JL, Gordeev I, Harty B, Heitner JF, Kenwood CT, Lewis EF, O'Meara E, Probstfield JL, Shaburishvili T, Shah SJ, Solomon SD, Sweitzer NK, Yang S, McKinlay SM, Investigators TOPCAT. Spironolactone for heart failure with preserved ejection fraction. *N Engl J Med* 2014; **370**: 1383–1392.
183. Chappell D, Jacob M, Hofmann-Kiefer K, Bruegger D, Rehm M, Conzen P, Welsch U, Becker BF. Hydrocortisone preserves the vascular barrier by protecting the endothelial glycocalyx. *Anesthesiology* 2007; **107**: 776–784.
184. Broekhuizen LN, Lemkes BA, Mooij HL, Meuwese MC, Verberne H, Holleman F, Schlingemann RO, Nieuwdorp M, Stroes ESG, Vink H. Effect of sulodexide on endothelial glycocalyx and vascular permeability in patients with type 2 diabetes mellitus. *Diabetologia* 2010; **53**: 2646–2655.
185. O'Connor CM, Starling RC, Hernandez AF, Armstrong PW, Dickstein K, Hasselblad V, Heizer GM, Komajda M, Massie BM, McMurray JJV, Nieminen MS, Reist CJ, Rouleau JL, Swedberg K, Adams KF, Anker SD, Atar D, Battler A, Botero R, Bohidar NR, Butler J, Clausell N, Corbalán R, Costanzo MR, Dahlstrom U, Deckelbaum LI, Diaz R, Dunlap ME, Ezekowitz JA, Feldman D, Felker GM, Fonarow GC, Gennevois D, Gottlieb SS, Hill JA, Hollander JE, Howlett JG, Hudson MP, Kociol RD, Krum H, Laucevicius A, Levy WC, Méndez GF, Metra M, Mittal S, Oh B-H, Pereira NL, Ponikowski P, Tang WHW, Tanomsup S, Teerlink JR, Triposkiadis F, Troughton RW, Voors AA, Whellan DJ, Zannad F, Califf RM. Effect of Nesiritide in Patients with Acute Decompensated Heart Failure. *New Engl J Med* 2011; **365**: 32–43.
186. Lu B, Figini M, Emanueli C, Geppetti P, Grady EF, Gerard NP, Ansell J, Payan DG, Gerard C, Bunnett N. The control of microvascular permeability and blood pressure by neutral endopeptidase. *Nat Med* 1997; **3**: 904–907.
187. Yun J-H, Koh YJ, Jeong H-S, Lee D-H, Lee EH, Cho C-H. Propranolol increases vascular permeability through pericyte apoptosis and exacerbates oxygen-induced retinopathy. *Biochem Biophys Res Commun* 2018; **503**: 2792–2799.
188. Taherzadeh M, Das AK, Warren JB. Nifedipine increases microvascular permeability via a direct local effect on postcapillary venules. *Am J Physiol Heart Circ Physiol* 1998; **275**: H1388–H1394.
189. Mentzer GG, Verhaert D, Giri S, Emani S, McCarthy B, Simonetti OP, Raman SV. Myocardial edema by noncontrast T2 mapping is increased in acute decompensated heart failure. *J Card Fail* 2012; **18**: S22.
190. Monmeneu JV, Bodí V, Sanchis J, López-Lereu MP, Mainar L, Núñez J, Chaustre F, Rumiz E, Chorro FJ, Llácer Á. Cardiac magnetic resonance evaluation of edema after ST-elevation acute myocardial infarction. *Rev Esp Cardiol* 2009; **62**: 858–866.
191. Kidambi A, Mather AN, Swoboda P, Motwani M, Fairbairn TA, Greenwood JP, Plein S. Relationship between myocardial edema and regional myocardial function after reperfused acute myocardial infarction: an MR imaging study. *Radiology* 2013; **267**: 701–708.
192. Fehrmann A, Treutlein M, Rudolph T, Rudolph V, Weiss K, Giese D, Bunck AC, Maintz D, Baeßler B. Myocardial T1 and T2 mapping in severe aortic stenosis: potential novel insights into the pathophysiology of myocardial remodelling. *Eur J Radiol* 2018; **107**: 76–83.
193. Jeserich M, Foll D, Olschewski M, Kimmel S, Friedrich MG, Bode C, Geibel A. Evidence of myocardial edema in patients with nonischemic dilated cardiomyopathy. *Clin Cardiol* 2012; **35**: 371–376.
194. Nishii T, Kono AK, Shigeru M, Takamine S, Fujiwara S, Kyotani K, Aoyama N, Sugimura K. Cardiovascular magnetic resonance T2 mapping can detect myocardial edema in idiopathic dilated cardiomyopathy. *Int J Cardiovasc Imaging* 2014; **30**: 65–72.
195. Amano Y, Aita K, Yamada F, Kitamura M, Kumita S. Distribution and clinical significance of high signal intensity of the myocardium on T2-weighted images in 2 phenotypes of hypertrophic cardiomyopathy. *J Comput Assist Tomogr* 2015; **39**: 951–955.
196. Amano Y, Yanagisawa F, Tachi M, Hashimoto H, Imai S, Kumita S. Myocardial T2 mapping in patients with hypertrophic cardiomyopathy. *J Comput Assist Tomogr* 2017; **41**: 344–348.
197. Vermes E, Pericart L, Pucheux J, Delhommais A, Alison D, Genee O. T2-

mapping and T1-mapping detect myocardial involvement in Tako-Tsubo cardiomyopathy: a preliminary experience. *J Cardiovasc Magn Reson* 2015; **17**: P354.
198. Scally C, Abbas H, Ahearn T, Srinivasan J, Mezincescu A, Rudd A, Spath N, Yucel-Finn A, Yuecel R, Oldroyd K, Dospinescu C, Horgan G, Broadhurst P, Henning A, Newby DE, Semple S, Wilson HM, Dawson DK. Myocardial and systemic inflammation in acute stress-induced (Takotsubo) cardiomyopathy. *Circulation* 2019; **139**: 1581–1592.
199. Liang Y-D, Xu Y-W, Li W-H, Wan K, Sun J-Y, Lin J-Y, Zhang Q, Zhou X-Y, Chen Y-C. Left ventricular function recovery in peripartum cardiomyopathy: a cardiovascular magnetic resonance study by myocardial T1 and T2 mapping. *J Cardiovasc Magn Reson* 2020; **22**: 2.
200. Kotecha T, Martinez-Naharro A, Treibel TA, Francis R, Nordin S, Abdel-Gadir A, Knight DS, Zumbo G, Rosmini S, Maestrini V, Bulluck H, Rakhit RD, Wechalekar AD, Gilbertson J, Sheppard MN, Kellman P, Gillmore JD, Moon JC, Hawkins PN, Fontana M. Myocardial edema and prognosis in amyloidosis. *J Am Coll Cardiol* 2018; **71**: 2919–2931.
201. Hulten E, Aslam S, Osborne M, Abbasi S, Bittencourt MS, Blankstein R. Cardiac sarcoidosis—state of the art review. *Cardiovasc Diagn Ther* 2016; **6**: 50–63.
202. Puntmann VO, Isted A, Hinojar R, Foote L, Carr-White G, Nagel E. T1 and T2 mapping in recognition of early cardiac involvement in systemic sarcoidosis. *Radiology* 2017; **285**: 63–72.
203. Augusto JB, Nordin S, Vijapurapu R, Baig S, Bulluck H, Castelletti S, Alfarih M, Knott K, Captur G, Kotecha T, Ramaswami U, Tchan M, Geberhiwot T, Fontana M, Steeds RP, Hughes D, Kozor R, Moon JC. Myocardial edema, myocyte injury, and disease severity in Fabry disease. *Circ Cardiovasc Imaging* 2020; **13**: e010171.
204. Gräni C, Eichhorn C, Bière L, Murthy VL, Agarwal V, Kaneko K, Cuddy S, Aghayev A, Steigner M, Blankstein R, Jerosch-Herold M, Kwong RY. Prognostic value of cardiac magnetic resonance tissue characterization in risk stratifying patients with suspected myocarditis. *J Am Coll Cardiol* 2017; **70**: 1964–1976.
205. Spieker M, Haberkorn S, Gastl M, Behm P, Katsianos S, Horn P, Jacoby C, Schnackenburg B, Reinecke P, Kelm M, Westenfeld R, Bönner F. Abnormal T2 mapping cardiovascular magnetic resonance correlates with adverse clinical outcome in patients with suspected acute myocarditis. *J Cardiovasc Magn Reson* 2017; **19**: 38.
206. Ferreira VM, Piechnik SK, Dall'Armellina E, Karamitsos TD, Francis JM, Ntusi N, Holloway C, Choudhury RP, Kardos A, Robson MD, Friedrich MG, Neubauer S. T1 mapping for the diagnosis of acute myocarditis using CMR: comparison to T2-weighted and late gadolinium enhanced imaging. *JACC Cardiovasc Imaging* 2013; **6**: 1048–1058.
207. Kotecha T, Knight DS, Razvi Y, Kumar K, Vimalesvaran K, Thornton G, Patel R, Chacko L, Brown JT, Coyle C, Leith D, Shetye A, Ariff B, Bell R, Captur G, Coleman M, Goldring J, Gopalan D, Heightman M, Hillman T, Howard L, Jacobs M, Jeetley PS, Kanagaratnam P, Kon OM, Lamb LE, Manisty CH, Mathurdas P, Mayet J, Negus R, Patel N, Pierce I, Russell G, Wolff A, Xue H, Kellman P, Moon JC, Treibel TA, Cole GD, Fontana M. Patterns of myocardial injury in recovered troponin-positive COVID-19 patients assessed by cardiovascular magnetic resonance. *Eur Heart J* 2021; **42**: 1866–1878.
208. Ojha V, Verma M, Pandey NN, Mani A, Malhi AS, Kumar S, Jagia P, Roy A, Sharma S. Cardiac magnetic resonance imaging in coronavirus disease 2019 (COVID-19): a systematic review of cardiac magnetic resonance imaging findings in 199 patients. *J Thorac Imaging* 2021; **36**: 73–83.
209. Weckbach LT, Curta A, Bieber S, Kraechan A, Brado J, Hellmuth JC, Muenchhoff M, Scherer C, Schroeder I, Irlbeck M, Maurus S, Ricke J, Klingel K, Kääb S, Orban M, Massberg S, Hausleiter J, Grabmaier U. Myocardial inflammation and dysfunction in COVID-19–associated myocardial injury. *Circ Cardiovasc Imaging* 2021; **14**: e012220.
210. Galea N, Marchitelli L, Pambianchi G, Catapano F, Cundari G, Birtolo LI, Maestrini V, Mancone M, Fedele F, Catalano C, Francone M. T2-mapping increase is the prevalent imaging biomarker of myocardial involvement in active COVID-19: a cardiovascular magnetic resonance study. *J Cardiovasc Magn Reson* 2021; **23**: 68.
211. Siddiqui Y, Crouser ED, Raman SV. Nonischemic myocardial changes detected by cardiac magnetic resonance in critical care patients with sepsis. *Am J Respir Crit Care Med* 2013; **188**: 1037–1039.
212. Ntusi N, O'Dwyer E, Dorrell L, Wainwright E, Piechnik S, Clutton G, Hancock G, Ferreira V, Cox P, Badri M, Karamitsos T, Emmanuel S, Clarke K, Neubauer S, Holloway C. HIV-1-related cardiovascular disease is associated with chronic inflammation, frequent pericardial effusions, and probable myocardial edema. *Circ Cardiovasc Imaging* 2016; **9**: e004430.
213. Torreão JA, Ianni BM, Mady C, Naia E, Rassi CH, Nomura C, Parga JR, Avila LF, Ramires JAF, Kalil-Filho R, Rochitte CE. Myocardial tissue characterization in Chagas' heart disease by cardiovascular magnetic resonance. *J Cardiovasc Magn Reson* 2015; **17**: 97.
214. Ntusi NAB, Piechnik SK, Francis JM, Ferreira VM, Matthews PM, Robson MD, Wordsworth PB, Neubauer S, Karamitsos TD. Diffuse myocardial fibrosis and inflammation in rheumatoid arthritis: insights from CMR T1 mapping. *JACC Cardiovasc Imaging* 2015; **8**: 526–536.
215. Greulich S, Mayr A, Kitterer D, Latus J, Henes J, Steubing H, Kaesemann P, Patrascu A, Greiser A, Groeninger S, Braun N, Alscher MD, Sechtem U, Mahrholdt H. T1 and T2 mapping for evaluation of myocardial involvement in patients with ANCA-associated vasculitides. *J Cardiovasc Magn Reson* 2017; **19**: 6.
216. Eyler AE, Ahmad FA, Jahangir E. Magnetic resonance imaging of the cardiac manifestations of Churg-Strauss. *JRSM Open* 2014; **5**: 2054270414525370.
217. Galea N, Rosato E, Gigante A, Borrazzo C, Fiorelli A, Barchetti G, Trombetta AC, Digiulio MA, Francone M, Catalano C, Carbone I. Early myocardial damage and microvascular dysfunction in asymptomatic patients with systemic sclerosis: a cardiovascular magnetic resonance study with cold pressor test. *PLoS ONE* 2020; **15**: e0244282.
218. Ntusi NA, Piechnik SK, Francis JM, Ferreira VM, Rai AB, Matthews PM, Robson MD, Moon J, Wordsworth PB, Neubauer S, Karamitsos TD. Subclinical myocardial inflammation and diffuse fibrosis are common in systemic sclerosis—a clinical study using myocardial T1-mapping and extracellular volume quantification. *J Cardiovasc Magn Reson* 2014; **16**: 21.
219. Abdel-Aty H, Siegle N, Natusch A, Gromnica-Ihle E, Wassmuth R, Dietz R, Schulz-Menger J. Myocardial tissue characterization in systemic lupus erythematosus: value of a comprehensive cardiovascular magnetic resonance approach. *Lupus* 2008; **17**: 561–567.
220. Zhang Y, Corona-Villalobos CP, Kiani AN, Eng J, Kamel IR, Zimmerman SL, Petri M. Myocardial T2 mapping by cardiovascular magnetic resonance reveals subclinical myocardial inflammation in patients with systemic lupus erythematosus. *Int J Cardiovasc Imaging* 2015; **31**: 389–397.
221. Gouya H, Vignaux O, Le Roux P, Chanson P, Bertherat J, Bertagna X, Legmann P. Rapidly reversible myocardial edema in patients with acromegaly: assessment with ultrafast T2 mapping in a single-breath-hold MRI sequence. *AJR Am J Roentgenol* 2008; **190**: 1576–1582.
222. Gao X, Liu M, Qu A, Chen Z, Jia Y, Yang N, Feng X, Liu J, Xu Y, Yang X, Wang G. Native magnetic resonance T1-mapping identifies diffuse myocardial injury in hypothyroidism. *PLoS ONE* 2016; **11**: e0151266.

223. Marie PY, Angioï M, Carteaux JP, Escanye JM, Mattei S, Tzvetanov K, Claudon O, Hassan N, Danchin N, Karcher G, Bertrand A, Walker PM, Villemot JP. Detection and prediction of acute heart transplant rejection with the myocardial T2determination provided by a black-blood magnetic resonance imaging sequence. *J Am Coll Cardiol* 2001; **37**: 825–831.
224. Vermes E, Pantaléon C, Auvet A, Cazeneuve N, Machet MC, Delhommais A, Bourguignon T, Aupart M, Brunereau L. Cardiovascular magnetic resonance in heart transplant patients: diagnostic value of quantitative tissue markers: T2 mapping and extracellular volume fraction, for acute rejection diagnosis. *J Cardiovasc Magn Reson* 2018; **20**: 59.
225. Alabed S, Saunders L, Garg P, Shahin Y, Alandejani F, Rolf A, Puntmann VO, Nagel E, Wild JM, Kiely DG, Swift AJ. Myocardial T1-mapping and extracellular volume in pulmonary arterial hypertension: a systematic review and meta-analysis. *Magn Reson Imaging* 2021; **79**: 66–75.
226. Arcari L, Engel J, Freiwald T, Zhou H, Zainal H, Gawor M, Buettner S, Geiger H, Hauser I, Nagel E, Puntmann VO. Cardiac biomarkers in chronic kidney disease are independently associated with myocardial edema and diffuse fibrosis by cardiovascular magnetic resonance. *J Cardiovasc Magn Reson* 2021; **23**: 71.
227. Kotecha T, Martinez-Naharro A, Yoowannakul S, Lambe T, Rezk T, Knight DS, Hawkins PN, Moon JC, Muthurangu V, Kellman P, Rakhit RD, Gillmore JD, Jeetley P, Davenport A, Fontana M. Acute changes in cardiac structural and tissue characterisation parameters following haemodialysis measured using cardiovascular magnetic resonance. *Sci Rep* 2019; **9**: 1388.
228. Hayer MK, Radhakrishnan A, Price AM, Baig S, Liu B, Ferro CJ, Captur G, Townend JN, Moon JC, Edwards NC, Steeds RP. Early effects of kidney transplantation on the heart—a cardiac magnetic resonance multi-parametric study. *Int J Cardiol* 2019; **293**: 272–277.
229. Hayer MK, Radhakrishnan A, Price AM, Liu B, Baig S, Weston CJ, Biasiolli L, Ferro CJ, Townend JN, Steeds RP, Edwards NC, Birmingham Cardio-Renal Group. Defining myocardial abnormalities across the stages of chronic kidney disease: a cardiac magnetic resonance imaging study. *JACC Cardiovasc Imaging* 2020; **13**: 2357–2367.
230. Thavendiranathan P, Amir E, Bedard P, Crean A, Paul N, Nguyen ET, Wintersperger BJ. Regional myocardial edema detected by T2 mapping is a feature of cardiotoxicity in breast cancer patients receiving sequential therapy with anthracyclines and trastuzumab. *J Cardiovasc Magn Reson* 2014; **16**: P273.
231. Damman K, Gori M, Claggett B, Jhund PS, Senni M, Lefkowitz MP, Prescott MF, Shi VC, Rouleau JL, Swedberg K, Zile MR, Packer M, Desai AS, Solomon SD, McMurray JJV. Renal Effects and Associated Outcomes During Angiotensin-Neprilysin Inhibition in Heart Failure. *JACC Heart Fail* 2018; **6**: 489–498.